Aalto-yliopisto
Aalto-universitetet
Aalto University

Master's Program in Advanced Energy Solutions

Simulation of a modified S-Graz cycle with AspenPlus

Alessandro Bonaveri

Master's Thesis
2023

Aalto-yliopisto
Aalto-universitetet
Aalto University

Author Alessandro Bonaveri

Title of thesis Title of your thesis

Programme Master in advanced energy solutions

Major Name of your major

Thesis supervisor Associated Professor Mika Järvinen

Thesis advisor Matthias Re

Date 17/07/2023 **Number of pages** 58+5 **Language** English

Abstract

To tackle the climate change, the shift to renewable sources is the primary answer, but it cannot be the only one due to their high intermittency. In countries like Italy, where the primary energy source is natural gas, fossil fuels will still play an important role in their energy mix. This work tries to present the Italian scenario and evaluate the performances of a modified S-Graz cycle, which couple fossil power plants with zero-emission energy. By keeping the combustion temperatures relatively low with flue gas recirculation and steam injection and by running with the oxy-combustion of natural gas, its flue gas mostly contain carbon dioxide and can theoretically be completely captured, releasing zero emissions in the atmosphere. To perform the calculations, a steady-state model of the cycle has been built in AspenPlus. The model revealed that the flue gas recirculation is source of significant losses, which greatly decrease the efficiency. In addition technological limits make the isolation of the oxygen, to use as comburent, and the purification of the flue gas highly energy intensive, further decreasing the efficiency. In this work, three modifications were proposed to increase the cycle efficiency. The simulations showed that by reducing the steam injection pressure and by optimizing the heat exchange within the cycle, the recirculated mass flow is reduced and an electrical efficiency of 44.2% is obtained. Such efficiency is lower than the conventional combine cycle gas turbine plants', but the complete flue gas carbon capture make the cycle a viable solution for the Italian energy transition. Further calculations on the effect of the fuel purity on the cycle performances were performed, but they showed that the cycle efficiency does not depends on the natural gas quality.

Keywords Oxy-combustion; S-Graz cycle; Italy.

Table of Contents

Preface 5
Abbreviations & Symbols 6
Abbreviations 6
Symbols 7
1.1 Objective 9
2.1 Carbon problem 11
2.2 EU green deal 12
2.3 Renewable energy 14
2.4 The Italian case 15
2.4.1 Italian energy production and emissions 15
2.4.2 Italian gas dependence and infrastructures 17
2.5 Carbon capture and storage 20
2.6 ASU 25
2.7 Graz cycle 27
2.8 Modified S-Graz cycle 29
2.8.1 Oxy-combustion 29
2.8.2 Gas turbine side 29
2.8.3 Flue gas condensation and injection side 30
2.8.4 Steam side 30
2.8.5 Carbon capture 30
3.1 Methods and hypothesis 31
3.2 Working conditions assumed 32
3.3 Base-case model description 34
3.3.1 Design improvements 40
4.1 Convergence solution 46
4.2 Efficiency analysis 47
4.3 Fuel effect 52
5 Conclusion 57
6 References 59

Preface

I want to thank Professor Järvinen Mika Supervisor and Matthias Re Advisor for their kindness and guidance. Professor Luciano Rolando for his willingness.

I also want to thank my parents for supporting me and giving me the chance to study abroad, my friends for the late nights spent together and my partner for being always by my side.

Otaniemi, 25 June 2023

Bonaveri Alessandro

Abbreviations & Symbols

Abbreviations

COP	Conference Of Parties
UNFCCC	United Nations Framework Convention on Climate Change
UN	United Nations
GHG	Green House Gases
IEA	International Energy Agency
EU	European Union
CCGT	Combined Cycle Gas Turbine
ASME	American Society of Mechanical Engineering
RES	Renewable Energy Source
EIA	U.S. Energy Information Administration
NG	Natural Gas
PNIEC	Piano Nazionale Integrato per l'Energia ed il Clima
TES	Total Energy Supply
LNG	Liquid Natural Gas
TAG	Trans Austria Gas
TRANSMED	TRANS MEDiterranean
TAP	Trans Adriatic Pipelina
OLT	Offshore LNG Toscana
STOGIT	STOccaggio Gas Italia
FSRU	Floating Storage Regasification Unit
HRSG	Heat Recovery Steam Generator
OCGT	Open Cycle Gas Turbine
CHP	Combined Heat and Power
CC	Carbon Capture
CCUS	Carbon Capture Utilisation and Storage
CM	Carbonaceous Materials
HT	Hydrotalcites
MOF	Metal-Organic Frameworks
RTI	Research Triangle Institute
NGCC	Natural Gas Combined Cycle plant
TFC	Thin-Film Composite
GPU	Gas Permeance Unit
MMM	Mixed Matrix Membranes
SCOC-CC	Semi-Closed Oxyfuel Combustion Combined Cycle
EOR	Enhanced Oil Recovery
ETS	Emission Trading Scheme
TSA	Temperature Swing Adsorption
PSA	Pressure Swing Adsorption
VPSA	Vacuum Pressure Swing Adsorption
ASU	Air Separation Unit
CPU	Compression and Purification Unit
DH	District Heating

Symbols

η_{net}	Net electrical efficiency
P_i	Net work required by the i^{th} component
LHV	Lower eating Value
ρ_{st}	Standard mass density at 15 °C, for a petroleum mixture
$\dot{q}_{st}$	Standard vapor volumetric flow at 15°C
P_{ideal}	Power ideally obtainable by the fuel
sm^3	Standard cubic meter
η_{cog}	Cogeneration efficiency
Q_{net}	Cycle net heat power

1 Introduction

In December of 2015, during the 21st Conference of the Parties (COP21) of the UNFCCC, it was drafted the Paris Agreement. The Paris Agreement legally binds the signing countries to an international treaty on climate change. 196 countries in the world signed the agreement and in 2016 it was officially validated. Today, the only major emitter in the world, that did not comply to the agreement is Iran.

The Paris Agreement main goal, is to limit climate change by keeping the increase of the average world temperature below 1.5°C compared to the pre-industrial temperature. According the United Nations, the climate change is a consequence of the pollutant emissions related by human activities, in particular fossil fuel combustion and industrial processes [1]. If no climate policies on this regard are implemented (business as usual), the average global temperature will increase beyond 1.5°C (respect to pre industrial levels). This will result in much more frequent and severe climate disasters, such as droughts, heatwaves and heavy rainfall [1].

UN considered multiple possible global pathways to counter climate change. In all the considered paths, where the temperature increase was successfully limited below 1.5°C, the Green House Gas emission peaked between 2020 and 2025, and averagely decreased of 43%, respect to 2019 levels, by 2030 [1]. All the solution pathways called for immediate GHG emission reduction policies. In 2022, the major source of GHG emissions in the world was the power sector (electricity and heat generation). As reported by the IEA, the power sector was responsible for 42% of global emissions, the industry and transport sectors for 26% and 23% respectively, while the emissions associated to buildings accounted for only 9% of the total [2]. It can be easily noticed how the most crucial sector to decarbonise is the power sector.

The European Union is following Its own pathway to tackle climate change. It takes the name of European Green Deal and consists in a set of policies that cover all sectors related to emissions, with the common objective of emitting net zero carbon emissions by 2050.

Decarbonisation can be reached in different ways. The main options for the power sector are increasing the share of carbon free sources (like renewable sources), improving the efficiency of the power generating processes or "catching" the produced emissions before their release in the atmosphere. In the EU, the strategy is decided by the government of each country and it depends on the resources and the infrastructures available in that country. In countries where there is a large power demand, renewable sources alone will not be able to meet it by 2050, their constant nature does not allow them to properly follow the sudden changes of the demand, especially during the daily peaks. To fill the gap between demand and renewable energy, storage systems can be used, but the materials needed for the construction of both the storage and production systems are expensive and limited. Therefore, even if the current and future policies will decrease the share of carbon

intensive technologies, they will still be used in the future. This is especially true in countries like Italy, where natural gas is the main source of energy. Since fossil based plants will still be used, Italy needs to focus on carbon capture systems in order to reduce the emissions of its power sector. Carbon capture systems used in the power sector decrease the emissions generated by the combustion of a fossil fuel and are divided among pre-, post- and oxy-fuel combustions. Pre-combustion extracts and captures the carbon content of a fuel through chemical reaction, before its combustion. Post-combustion exploits the fluid properties of the molecules present in the flue gas to extract the carbon dioxide. Oxy-fuel combustion utilizes pure oxygen as the comburent, so that the flue gas are, as much as possible, composed only of water and carbon dioxide.
Among these three methods, oxy-fuel combustion is the most effective in capturing the carbon, in power cycles it can capture even more than 99% of the carbon dioxide produced [3]. Oxy-fuel combustion can be implemented to almost any thermal cycle that requires combustion, it greatly limits the emissions, but the oxygen separation is very expensive and energy intensive [4]. Nevertheless, a valid pathway for Italy to contribute to the carbon neutrality objective, set by the European Union, is to implement oxy-combustion systems to its current natural gas turbines. The oxy-fuel thermodynamic cycles may require modifications to reduce the efficiency decrease because of the high energy consumption of the oxygen separation [5].
The Graz cycle is a particular CCGT that enhance the potential of oxy-fuel technology. The Graz cycle running on natural gas, is a complex combined cycle gas turbine characterized by oxy-fuel combustion, carbon capture, flue gas recirculation and steam injection. This kind of power plant would be able to cover a great part of the energy demand, while being able to adjust its power output and emitting almost zero pollutants. By burning natural gas with highly pure oxygen and by limiting the cycle temperatures through flue gas recirculation and steam injection, the only combustion product are water and carbon dioxide. Through heat recovery systems, the water in the flue gas is condensed while producing more power. As a result the carbon separation is mostly completed in the cycle and the flue gas can be captured as a whole, further carbon separation can be done in a further step.

1.1 Objective

The objective of the study is to evaluate the net electrical efficiency of a modified S-Graz cycle modelled owing to Aspen Plus software. The S-Graz cycle is a particular Graz cycle whose working fluid has a high steam content.
The Graz cycle principle was first published in 1985 for the combustion of hydrogen, in the ’90s was then adopted for the combustion of fossil fuels.

Since then, many studies and improvements have been done on the Graz cycle. This work focuses on a cycle layout proposed at ASME expo in 2006 for a 400 MW power plant [6].
The results are compared respect to other gas cycles currently in operation and to the results presented at ASME. This work does not analyse a real size plant, but focuses on the thermodynamic cycle considering a unitary mass flow of natural gas.

2 Literature review

2.1 Carbon problem

The effects of the climate change forced the United Nations to take countermeasures to limit the pollutant emissions of the human activities. With the Paris Agreement of 2015, the member states are legally bound to reduce the emissions that they generate. The objective is to avoid that the global temperature increase, caused by the climate change, may reach 1.5°C respect to pre-industrial levels. The UN declared that human activities are the cause of climate change and that the global temperature has already increased of 1.1°C, if it were to reach 1.5°C the number of weather and climate extreme events would increase even more [1]. While these events could directly arm humans, the atmosphere, the oceans, the cryosphere and the biosphere would be damaged indirectly. These changes would be the cause of extinction or endangerment of many species, such as pandas and polar bears, but also of may insects like bees, which would cause food famine. On the other hand the melting of the cryosphere will gradually reduce the potable water reserves. To take on the climate change the United Nations evaluated many global pathways. These pathways are divided into two groups, those that successfully limited the global warming below 1.5°C and those that were not successful, but focused on not going beyond the 2°C increase limit. Among the 2°C models, some of them consider an overshoot: the warming limit of 1.5°C is actually breached, but by increasing the number of carbon removal systems, the warming is decreased down to 1.5°C by 2050. In the successful models, the Green House Gases emission peaked between 2020 and 2025, and averagely decreased of 43%, respect to 2019 levels, by 2030. In the end, by 2050, GHGs averagely decreased of 84% respect to 2019 levels [1]. According to the UN's work, due to some hard-to-abate GHG sectors, such as agricultural, aviation and industrial sectors, net zero CO_2 emissions is reached before net zero GHGs [1].

In all the modelled pathways, successful and not, immediate and strong climate policies were required.

Table 1 shows the average percentage emissions reduction (plus the maximum and minimum decrease) of the successful and unsuccessful models respect to 2019 levels [1].

Table 1: pathways emissions reduction

		Reduction from 2019 emission level (%)			
		2030	2035	2040	2050
Limit warming to 1.5 °C (no overshoot)	GHG	43 [34-60]	60 [49-77]	69 [58-90]	84 [73-98]
	CO_2	48 [39-69]	65 [50-96]	80 [61-109]	99 [79-119]
Limit warming to 2°C	GHG	21 [1-42]	35 [22-55]	46 [34-63]	64 [53-77]
	CO_2	22 [1-44]	37 [21-59]	51 [36-70]	73 [55-90]

In March 2023, the International Energy Agency published its report on CO_2 emissions during 2022. The report analyses the GHGs emissions generated in 2022 by the energy related sectors. While most of the work focuses on CO_2, it also provides information on methane and NO_x emissions. The report states that the global energy-related CO_2 emissions grew by 0.9% respect to the previous year, reaching a new all-time high value of 36.8Gt, which is still not that high, considering the energy prices shocks and the changes of traditional fuel trades caused by the Ukrainian war [2]. IEA highlighted how the power and heat sector was the most carbon intensive energy related sector and accounted for 42% of the global emissions. It was also the sector with the biggest emissions increase from 2021 to 2022, with a percentage increase of 1.8%, reaching 14.6Gt of CO_2. The other sectors, the industry, transport and building sectors, were responsible for 26%, 23% and 9% respectively [2]. The power and heat sector is by far the most crucial sector to decarbonise.

2.2 EU green deal

In order to tackle the climate change, on the 11th of December 2019 the European Union presented a new set of proposals. These proposals take the name of European Green Deal and ensure that the member states will comply to the Paris agreement of 2015. The EU green deal promote an economic growth decoupled from the resource use, considering all the European citizens, with different capital and needs. The ultimate goal of these proposals is for Europe to emit 0 net green house gas emissions by 2050, becoming the first climate neutral continent in the world.

To make sure that the goals are reached, on the 17th of November 2020, the European commission presented the 2030 target plan, an halfway deadline to monitor the member states' progress.

By 2030 the GHG emissions must be reduced of 55% compared to the 1990 levels, which means a reduction of approximately 18% respect to 2020 levels (moment of the presentation of the target).

The proposals focus on all the energy sectors: transport; industrial; buildings; heat and power.

For the transport sector the objective is to reduce by 55% the emissions from cars by 2030, while from 2035 all the new cars on sale should produce zero emissions. The emissions reduction will not focus exclusively on cars, both the aviation and maritime transports will need to use cleaner fuels, for the aviation sector the restriction will apply to intercontinental flights taking off from EU ground as well [7].
The industrial sector will see the share of energy coming from renewables increase, with this, their products will earn green certificates, those without these certificates, especially extra-European companies operating in countries with less strict climate rules, will be subject to taxation. Thanks to the taxation, called carbon pricing, European companies will not be penalised by the transition to renewables and their products will be competitive on the market (at least in the European one) [7].
The building sector represent the 40% of European energy demand, most of it due to heating and cooling systems. To reduce the emissions from the sector the building efficiency should increase, so that they require less energy, and the energy consumed should come from renewables source. For private buildings, heavy incentives, meant to promote renovation, should permit the renovation of 35 million buildings in the whole Europe by 2030. The member states should also renovate 3% of the total public floor and increase the renewables usage for heating and cooling in all the buildings by 1,1% every year until 2030. In the end, by the same year, at least the 49% of the total energy demand from building should be satisfied by renewables [7].
Similar to the building sector, the proposals for the heat and power sector are meant to increase the energy production processes efficiency and the share of renewables in the energy production. The share of renewables should reach 40% of the total, while the efficiency should be between 36 and 39% [7].
With these proposals the emissions will be reduced, but not eliminated. To capture the CO_2 that will unavoidably still be emitted, plus the one that is already in the atmosphere, reforestation is a cheap option, therefore Europe plans to plant 3 million additional trees by 2030. Reforestation processes are able to recover the CO_2 already present in the atmosphere, but for some sectors, especially the heat and power sector, it is possible to capture at least part of the carbon dioxide produced before its release.
The energy transition, encouraged by the European Green Deal, is a process that will take many years to ultimate, in the meantime, carbon based energy will still be produced and maybe it will even after the Green Deal deadline (in 2050), after all, Europe is aiming to become carbon neutral not carbon free.

2.3 Renewable energy

The increase in share of renewable sources in a country's energy mix is the easiest pathway to reduce carbon emissions and reach the European target set by the Green Deal .

Renewable energy is energy that comes from a natural source that will not run out. They are derived from natural processes and are self-replenishing [8]. According to the United Nations, to be considered renewables their consumption rate has to be lower than their replenishing rate [9]. The most commonly addressed renewable energy sources are solar and wind power, hydroelectric, geothermal and bioenergy. At the moment, hydroelectric energy is the renewable source with the highest electric power production. However, since it generate power from the flow/fall of a water stream and is unlikely that new suitable water reserves will be found, among the RES, the most appealing electric energy source for future development, are the solar and wind power technology [9].

Renewable sources are present everywhere, but depending on the location some are stronger than others. For example, the north of Europe is more suited for wind power thank to its rather flat landscape and strong wind, while the south is generally more suited for solar power being it closer to the equator [10], [11].

Two of the biggest renewable energy systems advantages are the theoretically infinite supply and, since they are present everywhere, they reduce a country's foreign energy dependence. However, renewable energy technologies have geographical and production limitations. Geographical limitations reduce the number of possible installation sites, for example, is very hard to install a wind turbine on a mountain. Energy production limitations are caused by uncertainties in the magnitude of the source (wind speed and solar irradiance), which make the production highly random and intermittent [12], [13]. Even with the production intermittency, the unlimited source of energy decrease the overall market price of energy, but makes them unable to meet daily energy peak demands.

Energy peaks generally depends on the geographical position of the country and on the season (climate and weather). As registered by the EIA (U.S. Energy Information Administration) and Terna (the owner of the Italian electrical grid), in the northern hemisphere during the cold season there are usually two peak demands, one between 8 to 11 (morning peak) and one between 18 to 20 (evening peak), generally the morning peak is higher. In the warm season peaks are from 10 to 12 and from 14 to 17,the warm seasons peaks are usually higher than the cold seasons' ones, probably due to air conditioning systems [14], [15].

Due to the mismatch of energy demand and renewable energy production, there are many debates on how to fill this energy gap when needed. To avoid emissions, the most famous and idealistic solution to the problem would be the use of batteries. The batteries would store previously generated

renewable energy, and would release it when needed, keeping the emissions to zero. Unfortunately batteries require very expensive materials and processes to be built and are not very efficient at storing great quantities of energy.
Since batteries cannot be the only solution to the mismatch problem, every state is trying to fill the energy mismatch in different ways, based on their local resources and already existing infrastructures.
In particular this study will analyse a possible solution for the Italian case.

2.4 The Italian case

With the Green Deal, the EU gives member states targets to reach and proposals on how to reach them, but is up to the member state's governments to decide on a proper pathway. The pathway is decided based on many factors, such as the already existing energy mix, the infrastructures and the magnitude of the energy demand.
Like almost all the other European countries, Italy will have to increase the share of renewables in the energy mix to at least reach 40% by 2030. However, being one of the most energy consuming country in the continent (the 5th), the amount of energy, hence of emissions, that will still be generated through non renewable sources, will be (as an absolute value) very high, making it unable to achieve a net emissions reduction of 55%, respect to 1990 levels, by 2030 (as asked by the EU) [16], [17]. This is especially valid for Italy, where the biggest share of energy production of the heat and power sector comes from natural gas [18]. A large number of infrastructures, a dense distribution net and long-term supply contracts with other countries, make Italy a highly gas dependent country. Therefore, emission reduction strategies for gas-fired plant will have to be integrated in the pathway to carbon neutrality.

2.4.1 Italian energy production and emissions

In 2021, in Italy, natural gas supplied a total of 2.6 millions of TJ of energy, in the electricity and heat production sector (energy supplier), it generated 60.4 Mt of CO_2, corresponding to 20% of the total in the same year.
To follow the EU Green Deal directive and reduce emissions in the energy production sector, Italy plans to phase out coal by 2025. Italy plans to replace coal plants with new natural gas plants or increase the capacity of already existing ones. Even if both coal and natural gas are carbon based fuels, their emissions performances are quite different. Just by considering the emissions generated from the extraction, processing and transport of the fuels, natural gas is much less polluting than coal: even if the gas losses during drilling and piping, NG extraction and transport processes, are very pollutants, the emissions generated by mining and transport of coal are much higher. While natural gas is a mixture of different gases, but is mostly methane (CH_4),

there are many kinds of coal. A finer coal means less impurities and a higher amount of energy that can be extracted by burning it. The finest coal is the anthracite or "hard coal", while the coal with the lowest energy content is lignite [19]. If energy production processes are considered, burning lignite or anthracite generate respectively 0.36 and 0.34 kg of CO_2 per kWh produced, on the other hand, natural gas burnt in a CCGT, a kind of natural gas plant that could substitute the coal based plants, generates only 0.2 kg of CO_2per kWh [20].
In 2021 coal plants emitted 17 Mt of CO_2, the transition to natural gas would approximately halve these emissions, still producing the same amount of energy.
Biomass is also another carbon based fuel that could potentially substitute coal power plants. The advantages of the biomass is that it is a renewable fuel source, unlike fossil fuels, and its combustion theoretically generates zero emissions. The combustion of biomass releases in the atmosphere the exact amount of CO_2 that will be captured, through photosynthesis, by the next generation of planted biomass. If transport and biomass processing emissions are not considered, the net emissions of biomass are zero. The disadvantage of biomass respect to fossil fuels is its smaller energy content, containing already an oxygen atom (biomass general composition: CHO) it is considered "half-burnt" and therefore can release less energy during combustion. For this reason biomass power plants are mostly small-scale plants, their capacity generally goes from 20 to 35 MW, far from the 500MW of capacity that can be reached by fossil fuels power plants [21]. Another great disadvantage of biomass is that it requires an extreme land and agricultural management, if the next biomass generation does not extract the carbon dioxide from the atmosphere, the carbon intensity of biomass energy is higher than coal's.
On the 21st of January 2020, Italy presented the PNIEC, the government's plan on energy to reduce GHG emissions as required by the EU green deal. In a particular part of the plan, the PNIEC states, as previously said, that Italy plans to phase out carbon by 2025. As of today, the number of carbon power plant operating in Italy is 6, they are owned by Enel, A2A and EP Produzione (Fig.1) [22]. Their total gross capacity is slightly above 3 GW, with Brindisi Sud, Torrevaldaliga Nord and Fiume Santo being the plants with the highest capacity: around 660 MW.

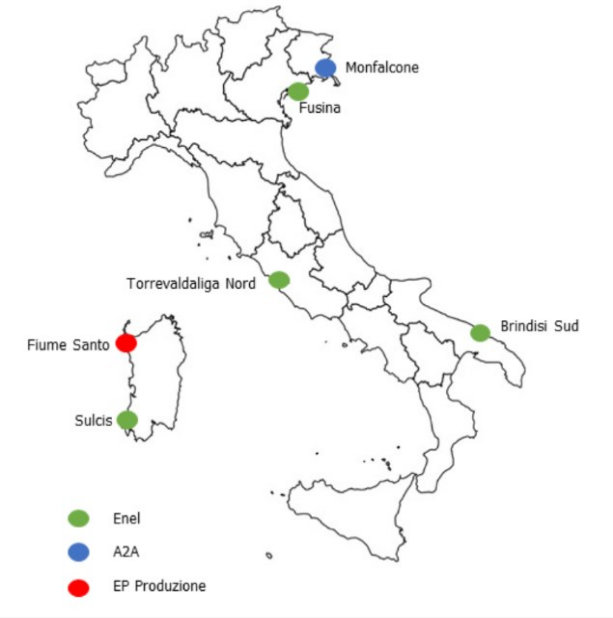

Fig. 1. Coal plants operating in Italy

The current share of energy produced by these plants will be substituted by 3 new additional GW of natural gas power plants capacity [23]. These 3 GW will come from either new plants or from empowering already existing ones. Another possible option, is to retrofit the coal-fired power plant transforming them into natural gas ones, this process is called brownfield transformation. The name indicates projects that do not start from scratch (greenfield), but are based on already existing infrastructures. The increase of natural gas capacity planned is compliant to the green target of the European Union (the carbon neutrality is reached considering the new emissions), however due to the decree on the capacity market, especially the part about the new power plant's premium, present in the same PNIEC, it is very probable that the number of natural gas plant will increase even more [23].

2.4.2 Italian gas dependence and infrastructures

The choice of natural gas to substitute coal is due to the great natural gas dependence of the country, both for heating and energy production.
In 2021 Italy consumed around 74 billion of cubic meter (Gm^3) of natural gas to produce energy, which correspond to 2.6 million of TJ and is approximately 43% of the total energy supply (TES) of the country [24]. On the other hand, if only the electrical energy is considered, the electricity generated from natural gas was 142 TWh, around 49% of the total electricity generated that year.

Even if Italy is the 11th country in the world with the highest natural gas consumption, It almost does not produce any on its own, most of the gas used comes from other countries [25].
This is possible thanks to a dense distribution network from the producers to the country and in the country Itself. The Italian natural gas infrastructures consist of 6 international pipelines (from other countries to Italy) and 3 LNG terminals.
Most of the national imported gas comes from the pipelines. At the moment there are 5 working international pipelines with a total capacity of 360 million of cubic meter per day (Fig. 2) [26]:

- The TAG: Trans Austria Gas pipeline brings the natural gas coming from Russia and enters Italy at Tarvisio. It is the pipeline with the biggest capacity in Italy and before the Ukrainian war used to carry 40% of the total Italian natural gas supply, but now it delivers only the 13% of the total supply [27].
- The TRANSMED: TRANS MEDiterranean pipeline, is an underwater pipeline that bring the Algerian gas to Italy (passing through Tunisia). It reach Italy in Sicily at Mazara del Vallo.
- The TRANSITGAS: is a Swiss pipeline that connect the Trans Europa Natural gas pipeline to the Italian gas network at Gries Pass owned by Snam Group. This bring the North-Western European gas to Italy, which is produced in the Netherlands and Norway.
- The GREENSTREAM: is a deep water pipeline that bring the gas from Lybia to Gela.
- The TAP: Trans Adriatic Pipeline is a pipeline that takes the Azeri natural gas from Turkey to the south of Italy, in Melendugno, passing through Greece and Albania.

The TAG has a side branch that pass through Slovenia before reaching Gorizia, but this branch is rarely used for imports, instead it is used to export the African gas or the LNG from Italian terminals to the Eastern Europe. A new pipeline called PCI is under construction, this pipeline will connect Slovenia to Hungary, increasing the possibility for Italy to become a natural gas supplier for Europe [28].
The 3 LNG terminals altogether have a import gas capacity of 54 million of cubic meters per day. They are located in Cavarzere (VE), Panigaglia (SP) and offshore near Livorno (LI). The biggest terminal, by far, is the Adriatic terminal, or Cavarzere, with an import capacity of 26.4 Mm^3 (million of cubic meter) per day, which correspond to almost 49% of the total, its regasification capacity is 8 Gm^3 per year. It is an offshore terminal, the first and only terminal, in Italy, that can accept gas from "super large scale vessels". Since the war in Ukraine, to reduce gas supply from Russia, a long-term LNG supply contract has been signed and now 80% of the annual regasification capacity of the terminal (approximately 6.4 Gm^3/y) is covered by Qatari gas.

The OLT near Livorno is another offshore terminal, while the Panigaglia terminal is onshore. The two LNG terminals have similar capacities, the OLT has a 15 Mm^3 daily capacity and 3.75 annual regasification capacity, while the Panigaglia terminal can receive 13 Mm^3 per day and supply 3.5 Gm^3 per year. To face possible crisis, maintain energy resilience and affordable prices, Italy

Fig. 2. Italian gas distribution net [26].

is equipped with many gas storage facilities. The total Italian storage capacity is 19.04 Gm^3. LNG terminals work as small gas storage facilities as well, but most of the stored gas is inside 13 underground storage sites, which are mostly depleted gas field. Depleted gas field are underground sand or rock formation that previously were a gas or oil reservoir. These storage field are state owned, but are operated by three main gas companies: Stogit, Edison and Ital gas.

Stogit, which is now part of the Snam group, is the biggest storage operator in Italy, it can store a total of 17.2 Gm^3, equal to 90% of the country's capacity.

On the other hand, Ital gas and Edison can store a maximum of 1 Gm^3 and 865 Mm^3 of gas respectively.
There are two kinds of stored gas, the commercial stocks, which are made available everyday to buyers via auction, and the strategic stocks, which are strictly regulated. Out of 19.04 Gm^3 of total gas capacity 4.6 Gm^3 are strategic stocks, Stogit controls almost all of them (4.48 Gm^3 which corresponds to 97% of all the strategic stocks), the rest is controlled by Edison (140 Mm^3). Strategic stock can only be used in particular conditions and for particular purposes. They can be released if the gas import (pipelines and LNG terminals) is at its maximum capacity and all the commercial storages have been depleted. The gas contained in the strategic stocks can only be used to supply households. The Italian strategic stocks are always full and they have never been released before.
The maximum gas withdrawal rate from storage is 329 Mm^3 each day, which corresponds to 1.7 days of demand (based on the daily average consumption in 2020). Therefore the Italian commercial gas reserves should last for approximately 74.6 days (without considering that demand depends on the season) under maximum withdrawal rate conditions.
To further reduce the gas supply from Russia and to better diversify the suppliers to avoid new potential gas crisis, Italian companies are working to further improve the natural gas infrastructure. Snam group, for example, will invest 9 billion euros, in the period between 2022 and 2026, to improve its infrastructure, of this amount, 1.3 billion will go expand the gas storage capacity; 6.3 billion will improve the pipeline transmission, especially the national Adriatic line, since the gas coming from the south will supply the north as well; 1.4 billion will be used to build offshore LNG terminals like Piombino and Ravenna FSRU (Floating Storage Regasification Unit) [29].
Even if natural gas is a carbon emitting energy source, all these investments can be justified because natural gas infrastructure could be relatively easily converted into hydrogen and ammonia infrastructure, therefore making the projects in line with the ongoing energy transition [30].

2.5 Carbon capture and storage

It is clear that Italy heavily relies on gas fuelled systems and plans to keep using them in the future. It then needs to implement proper emissions reducing systems to meets European standards, in order to achieve carbon neutrality. There exist three kinds of natural gas fired power plants: thermoelectric, gas turbine and the combined cycle gas turbine. Thermoelectric power plants generate electricity through a turbine that rotates with the flow of steam, the steam is generated from the evaporation of water that receives heat coming from the combustion of natural gas. Gas turbine plants act on the same principle, but the combustion of the gas takes place inside the turbine, therefore the mass flow in the turbine is not steam, but flue gas of the

combustion. CCGT are a combination of the two previous types, power is first generated by a gas turbine, when the hot flue gas exit the turbine, they exchange heat with a water stream in a HRSG, that then evaporates and expand in a secondary turbine like a thermoelectric plant, producing more power.
Thermoelectric power plants do not necessarily burn natural gas to run, they can also work by burning coal, oil or a co-feed of the three (for example gas with oil). There are many possible layouts for NG-fired power plants, therefore the efficiency ranges, which are also affected by the presence of auxiliary systems, are quite wide. For thermoelectric power plants the efficiency is generally between 35-45% [31]. For gas turbines, which are also called open-cycle gas turbine, the efficiency ranges between 20-35%, but the modern aeroderivative gas turbines can reach efficiencies of 33-43% [32], [33]. Respect to thermoelectrical plants, gas turbines have the advantage of not needing a large water source (like a river) because its working fluid is flue gas, but when they are working at a rated power lower than the nominal one their efficiency drop considerably [33]. By recovering the heat of the fluid coming out of the turbine with an heat exchanger, both this kind of plants can be converted into a CHP plant. CHP plants have generally higher efficiency and much lower fuel consumption (up to 40% of fuel saving) [34]. Among the gas-fired power plants, CCGTs are by far the most efficient and complex, their efficiency is approximately 60%, but, utilizing great amount of water as working fluid in the steam turbine, their installation has to be close to big water reservoir [35]. For this reason there have been some offshore installations, like in Norway, but these offshore plants met corrosion issues in the HRSG due to the use of salt water. Moreover, the efficiency of the offshore CCGTs is approximately 50% [35].
All the power plant considered generate flue gas from the combustion of natural gas and therefore produce CO_2 emission. The quantity is related to the amount of fuel burnt hence the plant efficiency, which is function of many factors, but generally is around the values presented above. For these kind of plants, the generation of CO_2 emissions is unavoidable. There are, however, ways to reduce the amount of CO_2 that is actually released in the atmosphere. In these processes the CO_2 is extracted from the combustion flue gas during the power plant operational time. The extraction takes the name of Carbon Capture and is one of the main solutions for the emission problem in sectors that are hard to decarbonise, such as the power sector. The proper name is CCUS and there are three different kind, specific for the power sector, or any sector that utilizes combustion processes, such as the industrial (except the automotive sector). These kinds differ based on the moment the CO_2 (carbon) is extracted: pre-combustion; post-combustion; oxy-combustion.
Pre-combustion processes separate the CO_2 from the fuel before that the combustion takes place. To do so, the fuel, typically coal or biomass, is made to react with air or oxygen to produce a synthetic gas, or syngas. This gas will be mainly composed by hydrogen, carbon monoxide and carbon dioxide. At

this point the carbon dioxide is extracted and the hydrogen present in the mixture will work as fuel for the combustion.
Post-combustion processes extract the carbon from the flue gas immediately after the combustion. This processes are currently the most widely used thanks to the fact that their implementation to the plant does not require many extra infrastructure.
The oxy-combustion process consist in the combustion of the fuel with highly pure oxygen, this is a carbon capture process itself, as the flue gas of such combustion will mostly contain CO_2 and water. In this case, the carbon dioxide does not need to be captured with any particular method: after an easy condensation of the water, all exhaust gas will consist of carbon dioxide.
The typical capture technique used are:

- Adsorption: carbon dioxide molecules are captured on the surface of a solid material upon contact. The adsorption requires particular temperature and pressure conditions to work efficiently. After being adsorbed, by reducing the pressure and increasing the temperature, the CO_2 is released again.
- Absorption: the working principle is the same as adsorption, the difference consists on the fact that the carbon dioxide is not captured on the surface, but dissolves in the material itself.
- Membrane separation: like in air separation processes, membrane separation exploit the differences in density and volatility between gases of the same mixture to separate them.
- Cryogenic separation: consecutive refrigeration and compressions to separate the flue gas components by taking advantage of their different condensation conditions [36].

With the climate change issue awareness growing everyday, there are and have been many studies concerning CC processes, in order to make them more efficient and economically convenient. Cryogenic separation is extremely energy intensive, due to high compression power and super low temperatures. As previously said, this process consists in a series of compressions and cooling with a column separation to obtain a CO_2-rich mixture. Therefore, the studies do not focus on technological innovations (on compressors or coolers) that can be applied, but instead they focus on the most optimal energy saving system that can be coupled, in order to diminish the energy expenditure of the CC. A particular study, for example, shows that by employing a heat integration system in the reboiler of the distillation unit, and by recovering the compressors' intercooling heat with an organic Rankine cycle, the energy requirement of a cryogenic separation system is reduced of approximately 22% [37].
Amine carbon absorption has proven as one of the best way to reduce carbon emissions. In low carbon flue gas, amine scrubbing showed 98% capture efficiency [38]. However it presents many drawbacks as it is limited to low

carbon streams (by increasing the carbon content of a stream the corrosion effect on the components increases), it requires high energy consumption for solvent regeneration and causes great efficiency reduction [38]. For these reasons, post-combustion adsorption is preferred to absorption (adsorbent regeneration is easier respect to solvent-based technologies) [39].
Studies on adsorption focus on developing adsorption materials with a faster regeneration and a higher capture efficiency in order to make this technology convenient (at the moment there are no commercial deployment of adsorption post-combustion capture technologies) [39]. The most studied adsorption materials are divided into zeolites, CMs , HTs and MOFs . Studies on zeolites materials analyse the adsorption capacity over a wide temperature range (between 25 and 877°C), in particular it has been studied the relationship between adsorption performances and crystal morphologies. Among the studied, nanosized morphologies showed the highest capture capacity of 70 $\frac{cm^3 CO_2}{g_{zeolite}}$. On the other hand, MOFs materials are the most suited for large-scale adsorption thanks to their high porosity, their adsorption capacity best the other materials, but unfortunately only in a temperature range between 0 and 30°C, quite low for flue gas temperature [40]. Among the adsorption materials HTs have shown the lowest adsorption capacity, but their working temperature is the highest as it range from 200 to 400°C [41]. To prove the efficiency of solid sorbent materials, the Research Triangle Institute carried out some bench-scale tests to simulate the CO_2 adsorption from flue gas generated by a natural gas combined cycle plant. The experiment consisted on "emitting" a variable flue gas mass flow rate (between 300 and 900 standard litre per minute $^{sl}/_{min}$) with a CO_2 concentration of 15 mol%. The adsorption material was a poly-ethylene mine that operated at 50-90°C. The results obtained by RTI showed that the adsorber was able to capture 90% of the CO_2 over a long period of time, but the adsorber was affected by fatigue: after 100 regeneration cycles the adsorption capacity dropped of 30% [42].
Among the CC systems, membrane separation is the one with the lowest energy drawbacks. Membranes are generally made of thin-film composite materials, which is able to separate by incorporating polar groups (separate molecules through their polarity), or nanoporous materials, which have extremely high gas permeability. The CO_2 permeance of this kind of membranes depends on many factors such as flue gas temperature, pressure and composition. Results published in literature for TFC membranes show that at pressure below 2 bar and at temperature between 25 and 100°C, the CO_2 permeance, expressed in GPU (how much gas pass through), was in the range 750-1100 and their $^{CO_2}/_{N_2}$ selectivity (how much of the gas that passed is CO_2) approximately averaged around the value of 30 [43]. Even though membrane separation is the most energy efficient CC system, it still needs improvements to become competitive [3]. It is currently being studied a new membrane

technology called Mixed Matrix Membrane, this membrane consist in a matrix of nanoporous material dispersed in polymers. The idea behind MMMs is to create a material that would combine the great gas permeability of the nanoporous materials, with the ability to separate molecules based on their polarity of the polymers (TFC) [44]. The technology is still at an early stage, but some promising results have been obtained: in some cases the CO_2 permeance reached 5000 barrer (which is equal to GPU times the thickness of the membrane) and with a selectivity respect to molecular nitrogen greater than 100 [45].
Since pre-combustion processes are not suitable for natural gas plants, they will not be analysed further.
On the other hand oxy-fuel combustion can be considered optimal for natural gas combustion: burning NG does not produce any sulphur byproduct or ash and by burning with almost pure oxygen, the NO_x emissions are very low as well. A study made in Hamburg compares the carbon capture performances obtained in a NGCC, by first using an amine based CC and then running it with oxyfuel combustion. The efficiency assumed for the NGCC was approximately 60%. By applying the absorber system, with a carbon capture efficiency of 90%, the efficiency is reduced of 7% (the biggest source of loss is the solvent regeneration) [46]. When oxyfuel combustion is applied, the NGCC requires some modifications: after exiting the HRSG the flue gas is further cooled and the water content is extracted, part of the flue gas is recirculated to cool down the temperatures. This plant is called SCOC-CC. The result obtained in the study show that the CO_2 was completely captured, but it required further "cleaning" since its concentration was not high enough (around 86 vol%) [46]. By relating the emissions captured in the two processes, with the amount of extra energy consumed with the two technique, it is shown that when high capture rate are required oxy-fuel combustion is more convenient than amine-based CC [46]. The main drawbacks of oxy-fuel are two, it requires great amount of energy, which make it non convenient at low carbon capture rates, and it cannot be applied to NG cycles without modifications and proper control techniques.
Once the carbon is captured, there are two possible options, it can be either stored, or utilised in other chemical processes (being stored does not necessarily means that it will not be used in a second moment). The storage of carbon dioxide usually means its injection into geological formations, like for some kind of storage facilities for natural gas [47]. On the other hand, there are many sectors where CO_2 can be utilised. At the moment, carbon can find its use in the cement and plastic manufacturing industry, in the EOR technique, in synthetic fuels and ammonia production processes and in the food industry [36] [48].
The downside of the carbon capture systems is the elevated cost, but international regulations are starting to make this kind of technology advantageous. In particular, the European ETS is limiting the amount of pollutants that can

be emitted in the atmosphere (in a particular area) while putting a price to them. The price of carbon is constantly rising, this will make carbon capture technologies increasingly cost-effective. Even more, if it is considered the fact that the captured carbon can be sold to carbon utilising companies.
When ETS is considered, among the carbon capture systems analysed, oxy-fuel combustion is the best choice, since it has the highest carbon capture ratio (100%), hence the smallest costs and the biggest revenues coming from carbon trading. For the same reason, if the objective is to maximize the emission reduction, to maybe compensate the emissions from sector that are harder to decarbonise, Italy should consider oxy-fuel CC to achieve carbon neutrality.

2.6 ASU

As previously said, oxy-fuel is highly energy intensive. Unlike the other CC systems, where generally the energy is required after the capture for regeneration, oxy-fuel requires great amount of energy for the production of the pure oxygen stream that works as comburent.
There are currently three main ways to produce streams with high concentration of oxygen: through cryogenic air separation, through swing adsorption or water electrolysis. Swing adsorption consist in the adsorption of the nitrogen present in the air with the help of a zeolite materials. There are two kinds of swing adsorption, TSA, where the zeolite is heated, or PSA, where the pressure of the air is decreased, among these, the VPSA can produce up to 300 tons of oxygen per day [49]. Swing adsorption does not require much energy, but the stream purity is limited to 94% [50].
When higher purity and higher production want to be achieved, cryogenic air separation is used. Generally called cryogenic ASU or cryogenic distillation, it is a system that is used for large-scale production of highly pure oxygen. An oxygen stream is considered highly pure when it is composed for at least 95% of O_2, cryogenic air separation can achieve purity up to 99% [50]. A NG power plant would definitely require large quantities of oxygen during its operation, therefore an ASU is required. While great quantities would assure constant plant operation, purity is also an important factor: in the combustion of natural gas, the concentration of nitrogen in the comburent is directly related to the amount of NO_x generated. Therefore, the use of an ASU reduces the NO_x emissions.
Cryogenic distillation exploits the liquefaction of oxygen for its extraction. The ambient air is extracted and cooled before entering a double column structure. The two columns are placed one on top of the other and are thermodynamically linked. The lower one, the high pressure one, is constantly fed by the cooled air and has a condenser at its top, the upper column, the low pressure one, has no condenser, but at its bottom has a reboiler (thermodynamically connected to the lower column condenser). The condenser of the

lower column liquify the air, the liquid is fed to the upper column, there, by taking advantage of the difference in the boiling temperature between oxygen and nitrogen (nitrogen has a lower boiling temperature), the heat from the reboiler evaporates the nitrogen. As a result, gaseous nitrogen exit the upper column from the top, while liquid oxygen is stored, and then extracted, at its bottom[5]. A recirculation system between the two columns enhance the efficiency and the products quality of the system. Generally the cryogenic distillation units use the double columns technique, but there are many studies on single- and multi-column cryogenic distillers.

The main focus of the studies is to reduce the energy consumption of the separation while maintaining a certain stream quality (oxygen purity). In the studies the target purity is generally fixed at 95%. A study conducted by the Washington University on a single-column ASU designed by Praxair, aims to reduce the production cost and improve the flexibility. The flexibility of an ASU is the ability to rump up or down the production based on minute-by-minute demand, which, in case of power plants, responds to the energy demand. The study showed that, for oxygen purity below 95%, the studied ASU brought great energy savings due to a much lower working pressure, respect to a conventional double-column ASU and a single-column ASU designed by Linde (a German company well established in the industrial gases sector). However, when the required oxygen purity is higher than 96% the double-column ASU is more energy efficient. The advantage of the single-column resides in the lower capital cost (it does not need a high pressure column) and in the faster start-up. Oxy-fuel combustion plants are not yet commercially available, at the moment ASUs are used for chemical separation in industrial processes and therefore deliver the products at particular conditions required by said processes. Industrial processes utilizes, for example, pure liquid nitrogen, which is not used in a combustion power plant. The University of Tokyo studied a single-column ASU based on self-heat recuperation, designed for oxy-combustion power plants. The idea is to exchange heat between the recirculating nitrogen coming from the top of the column with the liquid 0_2 stream entering the column as the bottom feed. Before the exchange, the nitrogen is compressed to increase its boiling temperature, while on the other hand the oxygen is decompressed in order to lower the boiling temperature, the pressures are adjusted so that the nitrogen boiling temperature is higher than the oxygen's. The results obtained by the study show that, with self-heat recovery, while producing an oxygen stream of 95% purity, the required energy for oxygen separation is 20.2% lower respect to a conventional double-column cryogenic ASU [5].

A promising technology for 0_2 production is electrolysis separation of water. With electrolysis separation the oxygen purity is 100%. Considering the water molecular composition, electrolysis is best suited for pure hydrogen production, the pure oxygen stream is considered a byproduct [50]. The main advantages of electrolysis are the use of electricity for the separation, making

it a possible destination for excess electricity (power-to-x), and the fact that the demand of hydrogen, as the cleanest fuel, is expected to increase. Even though electrolysis separation is a very promising technology, it is currently not suited to provide pure oxygen for oxy-combustion, it has been simulated that a renewable driven electrolyser consumes at least 4.3 MWh per ton of O_2 produced. In the case studied, the oxy-fuel combustion of a large scale coal power plant of 550 MW_e, required approximately 130 kg/s of oxygen. Electrolysis cannot produce fast enough to meet such O_2 demands [51]. In addition, the energy requirements would be bigger than the energy produced by the plant. Further improvements on electrolysers energy consumption have to be made for it to become a oxygen source for MW-scale plants [51].
At the moment cryogenic distillation is the only commercialized oxygen producing technology with big enough production capacity (bigger than 4000 tons of O_2 per day) [51].

2.7 Graz cycle

As previously said, oxy-fuel combustion cannot be immediately applied to any power plant, they first need to be modified. Some cycles have been specifically designed for oxy-combustion. They consider the different combustion performances and better exploit the flue gas composition. Among these cycles the Graz cycle is a NG combustion cycle with great performances [52]. The Graz cycle is a Combined Cycle Gas Turbine with steam injection and partial flue gas recirculation, powered by the oxy-fuel combustion of natural gas. The Graz cycle idea was developed in Japan in 1985, the creator first designed it for the stoichiometric oxy-combustion of hydrogen [53]. After some years, the hydrogen was set aside and the Graz cycle became a fossil-fired cycle. Since then many studies have been conducted on the cycle.
A study presented by the Graz University compares the performances of the NET power cycle (Allam cycle) and the Graz cycle. Both cycles run with oxy-combustion of natural, the main characteristics of the NET cycle are the extremely high combustion pressure (around 300 bar) and its working fluid, which is basically only CO_2 because the water is extracted before the flue gas recirculation [54]. The cycles are compared through thermodynamic analysis carried out with IPSEpro v7, which is a model used for modelling analysing and simulations of processes in power engineering. The results obtained from the modelling showed that the Graz cycle operates with better efficiency, between 52.2% to 53.5% (the efficiency calculations take into consideration the energy needed to produce oxygen and compress CO_2), and a higher volume flow rate at the turbine inlet, respect to the NET cycle [54].

In 2006 at ASME expo, it was presented the study of a modified S-Graz cycle that enhanced the heat recovery coming from the condensation of the flue gas. In this particular cycle the gas turbine is coupled with a low pressure Rankine cycle that receives the heat, through a series of heat exchangers, from the gas turbine flue gas that are not recirculated. During the heat exchange, the water content of the flue gas is condensed and separated, increasing the carbon dioxide concentration in the flue gas and easing up its separation and storage. As in a base Graz cycle, the water condensed from the flue gas is pressurized and then superheated in the HRSG, said water receives the heat from the gas turbine flue gas before its separation (one part is recirculated the other one gives the heat to the Rankine cycle). The superheated water is partially expanded in a high pressure turbine and the vapor coming out is injected in the gas turbine components. The "S-" prefix in the name indicates that the cycle working fluid has high water vapor content, as the "S" stands for steam. Fig. 3 shows the principle flow scheme of this particular Graz cycle.

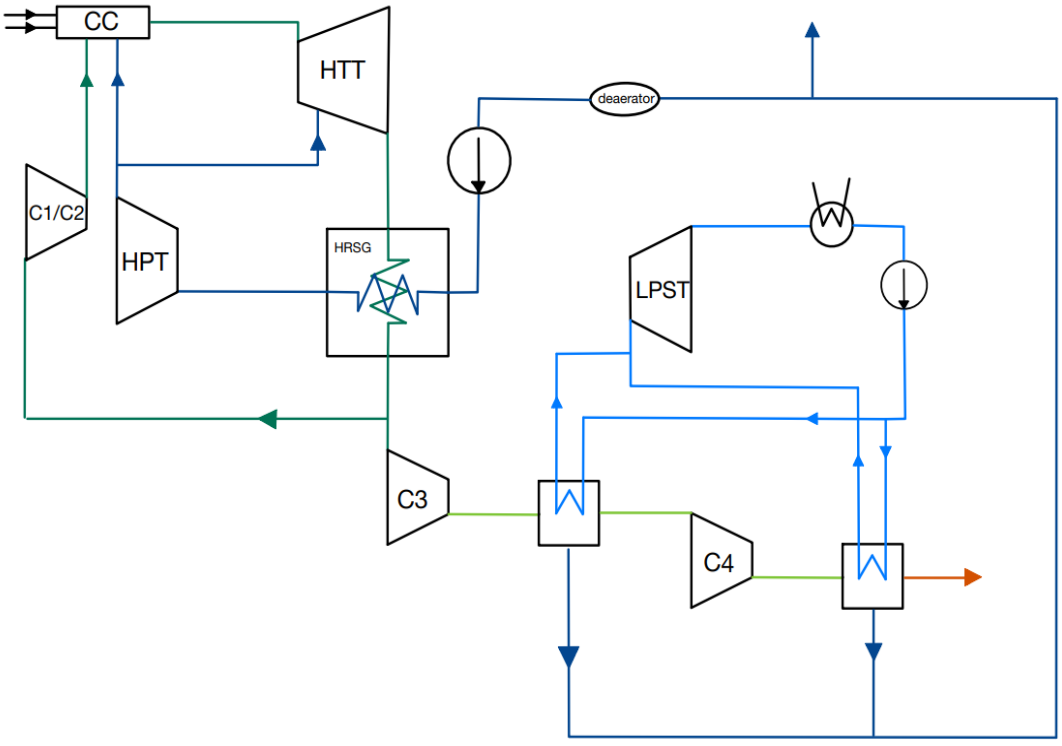

Fig. 3. Principle flow scheme of the modified S-Graz cycle

As shown in the figure, the cycle can be divided into 3 main parts based on the function and stream composition: The gas turbine side of the cycle; The steam side of the cycle; The flue gas condensation and injection. The different parts are highlighted by different colours: dark green streams represent the gas turbine side; the light blue represent the steam side; the light green

represent the flue gas condensation and the dark blue represent the water injection.
In the study, the author analysed the effects of flue gas condensation in a pressure range of 1 bar, by using a low pressure Rankine cycle as cooler. With the additional Rankine cycle (not present in the basic Graz cycle layout) and a proper machinery selection, the author declares that this modified S-Graz cycle can achieve net efficiency higher than 53% [55].
This study aims to evaluate the performances of the modified S-Graz cycle abovementioned and to validate its possible deployment in Italy.
The cycle choice is made considering the technological results found in the literature, the resource availability in the country and the emission targets set by the European Union.

2.8 Modified S-Graz cycle

2.8.1 Oxy-combustion

The combustion that takes place in the GT side of the cycle is an oxy-fuel combustion. This means that nitrogen oxide emissions are greatly reduced and the main combustion products of the oxy-fuel combustion of natural gas are carbon dioxide and water. Therefore, the mixture present in the combustion chamber is mainly composed of carbon dioxide and steam from the flue gas, steam from the steam injection, methane (NG) and oxygen. The amount of oxygen in the chamber is almost at stoichiometric level for the combustion of the natural gas, this is to keep the amount of extra oxygen as low as possible, thus decrease the combustion temperature [56]. This is the opposite respect to standard combustions which use normal air: since nitrogen does not contribute to the combustion, increasing the amount of air reduces the combustion temperature [57].
At the moment the cryogenic distillation is the most reliable and convenient technique for air separation, therefore it is assumed, that the highly pure oxygen needed for the S-Graz cycle's oxy-fuel combustion is the product of this particular plant.

2.8.2 Gas turbine side

The GT (gas turbine) side start with the feed of the natural gas and highly pure oxygen into the combustion chamber. When the combustion is completed, the flue gas enter the gas turbine and are expanded, afterwards they cede their remaining heat to the HRSG. The cooled flue gas are divided into two, part of it is recirculated while the other part goes into the "flue gas condensation and injection" side of the cycle. The flue gas recirculation is made of a series of two compressors that bring them back to the combustion chamber pressure. An intercooler between the two compressors make the process

easier by decreasing the flue gas temperature. The repressurized flue gas enters once again the combustion chamber closing the loop.

2.8.3 Flue gas condensation and injection side

The part of the flue gas that is not recirculated, enters a series of compressors and heat exchangers, whose task is to extract the biggest possible quantity of water from the gas themselves, through condensation. What is obtained are a condensed water stream and a cooled flue gas mostly containing carbon dioxide. The flue gas is extracted and exit the cycle, on the other hand the condensed water is only partly extracted. The non extracted part is purified with the use of a deaerator in order to remove impurities that would damage the components. The pure water is then pumped at high pressure into the flue gas HRSG (of the gas turbine side of the cycle), where it evaporates. The steam produced enters a steam turbine where is partially expanded, afterwards it is injected in both the combustion chamber and in the gas turbine of the GT side of the cycle.

2.8.4 Steam side

The steam side of the cycle is a low pressure Rankine cycle “separated” from the rest of the cycle, as it only receives heat from the condensation side. The feed of the cycle is extremely low pressure pure water, that is pumped into the heat exchangers of the condensation side of the cycle, where it evaporates. The steam then enters a low pressure steam turbine, where is expanded to the pressure of the feed water. Before returning as the Rankine cycle feed, it is cooled down until is fully condensed.

2.8.5 Carbon capture

The cooled flue gas exiting the cycle are mainly composed by carbon dioxide, water and nitrogen, merit of the oxy-combustion. The high percentage composition of carbon dioxide in the mixture, facilitates its extraction from the mixture itself, this avoid its release in the atmosphere.

3 Research materials and methods

In order to verify if the S-Graz cycle is really able to produce great amount of energy with reduced emissions (in line with the European energy transition), with the same level of efficiency of other similar technologies, the cycle has been modelled with the help of Aspen Plus. Aspen Plus is a chemical process optimization software for the design, operation and optimization of manufacturing facilities [58]. The version of the software used is the "v12.1" version. With Aspen Plus it has been studied the steady state operation of the cycle in function of the amount of natural gas used.
The results of interest are the composition of the gas exiting the cycle to see if they are "good" enough to be stored or released in the atmosphere; the amount of electrical power produced by the cycle based on how much power could be extracted by the fuel;

3.1 Methods and hypothesis

The model of the S-Graz cycle has been analysed using the Peng-Robinson equation of state as base method for the streams conditions. In case of free water, the method considered was the STEAM-TA method with a water solubility of 3.
To simplify the model, some hypothesis have been considered:

- The plant can perfectly control the process stream flows, being it a steady state calculation it is assumed that the various streams can travel in the pipes and in the components without any issue or delay at a constant mass flow;
- The pressure losses in the components are neglected, pressure losses are, for example, typically present in the heat exchangers, the streams would then require an increased pumping pressure;
- The inlet streams have constant state conditions (temperature and pressure) and constant composition (molar fraction), this is particularly important for the fuel inlet, where a change in composition can results in a different amount of extractable power, hence a different efficiency;
- All the heat exchangers in the cycle are fairly advanced and can operate with a minimum temperature difference between hot and cold streams of 1°C ($\Delta T_{min} = 1$).
- The isentropic and mechanical efficiencies of all the turbines and the compressors of the cycle have been considered constant, $\eta_{isentropic} = 0.8$, $\eta_{mechanical} = 0.95$. The efficiencies are related to the kind of turbine used, the choice of a turbine depends on many factors, one of them is the amount of power that said turbine is supposed to produce. Being the study focused on the production per unit of fuel entering the cycle, it is not known the exact amount of power that could be

generated, therefore the efficiencies chosen are not related to any particular kind of turbine. Even though the turbines in the cycle are not in the same range of power.

The results and the properties of all the streams of the cycle's simulation have been quantified using the default settings for the International System unit of measurement SI, with some modifications: the temperatures have been calculated in Celsius degrees instead of Kelvin and the power needed, produced or exchanged by the various components of the cycle was measured in Megawatts instead of Watts. Similarly to the power, the energy was measured in Megajoules instead of Joules. Therefore, the unit of measurement of the most used parameters and results are: mass flow rate [kg/s]; pressure [bar]; temperature [°C]; energy [MJ]; power [MW]. The streams composition has been expressed in molar fraction [mol%].

To complete the set-up of an Aspen Plus model, it is necessary to declare the chemical components that are present or could be formed during the simulation. In this case the only components that are present are the reagents and the products of the combustion of the natural gas. The components considered are listed in Table 2.

Table 2. Model components

IUPAC name	**Molecular formula**
Oxygen	O_2
nitrogen	N_2
Argon	Ar
Methane	CH_4
Ethane	C_2H_6
Propane	C_3H_8
n-butane	C_4H_{10}
Water	H_2O
Carbon dioxide	CO_2
Nitrogen dioxide	NO_2
Carbon monoxide	CO

3.2 Working conditions assumed

The cycle analysed is a particular modified version of the S-Graz cycle, the particularity of this cycle, respect to the non modified one, is that the working

fluid of the steam side of the plant go through condensation and evaporation at pressures below 1 bar.
To simulate the cycle, some stream conditions have been fixed based on previous studies [55].
For the gas turbine side of the cycle (Table 3):

1. Pressure of the combustion chamber;
2. Temperature of the flue gas entering the turbine;
3. Pressure of the flue gas exiting the turbine;
4. Temperature of the flue gas exiting the turbine;
5. Temperature of the flue gas exiting the HRSG;
6. Temperature of the flue gas after the series of compression (C_1/C_2).

Table 3. Fixed conditions: gas turbine side

Fixed condition	Component	Value
1	Combustion chamber	$P_{CC} = 40$ bar
2	Turbine inlet	$T_{HTT_{in}} = 1400$ °C
3	Turbine outlet	$P_{HTT_{out}} = 1$ bar
4	Turbine outlet	$T_{HTT_{out}} = 573$ °C
5	HRSG outlet	$T_{HRSG_{out}} = 180$°C
6	C_1/C_2 outlet	$T_{C_1/C_2} = 580$°C

For the condensation and injection side of the cycle (Table 4):

1. Pressure after the compressor C_3;
2. Pressure after the compressor C_4;
3. Temperature after the HRSG (water side);
4. Pressure after the HRSG (water side);

Table 4. Fixed conditions: recirculation and injection side

Fixed condition	Component	Value
1	Compressor C_3	$P_{C_3} = 1.27$ bar
2	Compressor C_4	$P_{C_4} = 1.95$ bar
3	HRSG outlet (water side)	$T_{HRSG,w_{out}} = 550$°C
4	HRSG outlet (water side)	$P_{HRSG,w_{out}} = 180$ bar

Lastly, for the steam side of the cycle (Table 5):

1. Evaporation pressure;
2. Temperature of the steam entering the turbine;
3. Condenser pressure.

Table 5. Fixed conditions: steam side

Fixed condition	Component	Value
1	Pump outlet	$P_{eva} = 0.75$ bar
2	Turbine inlet	$T_{LPST_{in}} = 175°C$
3	Condenser	$P_{cond} = 0.021$ bar

All the values fixed in the simulation are summarized in the following picture (Fig. 4) [55].

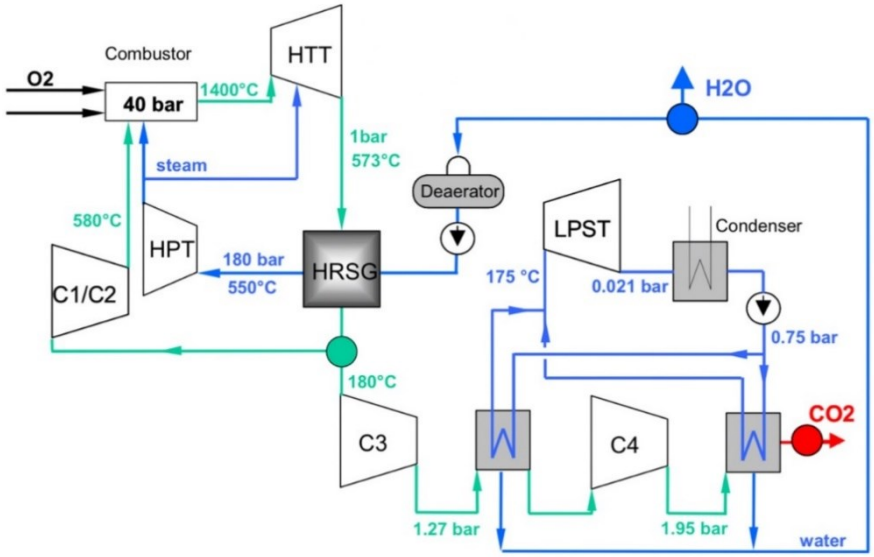

Fig. 4. Modified S-Graz cycle parameters

3.3 Base-case model description

Gas turbine side

The inlet flow of the cycle are the natural gas and the highly pure oxygen that will react with each others in the combustion chamber. The oxygen flow conditions use the results obtained by a standard cryogenic double column air separation unit after the oxygen is heated up in its main heat exchanger. The ASU takes ambient air (N_2 78 mol%;O_2 21 mol%; Ar 1 mol%) at a temperature of 25°C and pressure of 1 bar and produce a highly pure oxygen stream with a pressure of 15 bar and a temperature of 23°C [4]. Its composition is 95 mol% of molecular oxygen (around the lowest value to be considered highly pure), 1 mol% of molecular nitrogen and 4 mol% of argon.

On the other hand the molar composition of the natural gas entering the cycle, is based on the minimum gas quality standards, given by Snam Group and set by TAG GmbH. These standards are valid for all the gas sold in the

country by Snam Group starting from the 1st October 2022 until the same day of the next year [59]. The gas composition is as follows: methane (CH_4) 85 mol%, ethane (C_2H_6) 5 mol%, propane (C_3H_8) 3 mol%, butane (C_4H_{10}) 3 mol%, carbon dioxide (CO_2) 2 mol% and molecular nitrogen (N_2) 2 mol%. The pressure of the gas stream is 11 bar.

The mass flow of the natural gas stream is set to be constant and equal to 1 kg/s, on the other hand the mass flow of the oxygen is calculated in the simulation and is set so that it is obtained an almost stoichiometric combustion of the gas: molar fraction of oxygen in the flue gas equal to 0.1 mol%. As previously said this will limit the temperature of the flue gas. To calculate the appropriate value, an Aspen Design Spec (O2IN) is used, the oxygen flow rate is changed until the desired concentration is reached.

Before entering the combustion chamber, two compressors (C-GAS and C-O2), one each stream, increase the gas and oxygen's pressure up to 40 bar. The combustion chamber is simulated by an Aspen RGibbs reactor, it operates at a pressure of 40 bar and is considered adiabatic. The number of streams entering the chamber are in total 4: the two cycle input (the gas and the oxygen), the injected steam (stream: COMB-VAP), from the condensation and injection side of the plant, and the recirculated flue gas (stream: REC-4). The RGibbs is used for multi-phase reactions and is set to reach thermal and chemical equilibrium.

After the combustion, all the flue gas (newly generated flue gas, recirculated gas and injected steam), at a temperature of 1400°C, enter, with the rest of the injectable steam (stream: TURB-VAP), the high temperature turbine HTT. The turbine discharge the inlet streams at a pressure of 1 bar and their temperature goes down to 573°C. The discharged flue gas (stream: POST-HTT) enter the first Aspen HeatX (HRSG), which represent the heat recovery steam generator, where they are further cooled down to a temperature of 180°C by exchanging heat with water.

The flue gas (stream: POST-HRS) are then split into two (streams: COLD-FLU and REC-1) by an Aspen FSplit (FLUE-REC), part of it will head to the condensation and injection side of the cycle (stream: COLD-FLU), while the other part will remain in the gas turbine side of the cycle and will be recirculated into the combustion chamber. The recirculated part enters a series of two compressors (C_1 and C_2) divided by an intercooler. The two compressors increase the sub-stream pressure first up to 13 bar and then up to 40 bar (the combustion chamber's pressure). The intercooler cools down the temperature of the flue gas to facilitate their compression and to limit their temperature, the intercooling is controlled by a design spec (INTERCOO), which vary the intercooling temperature so that the temperature of the flue gas, entering the combustion chamber (stream: REC-4), is 580°C.

The flue gas split (FLUE-REC) as well, is controlled by a design spec. In this case, the controlled parameter is the stream splitting fraction, the parameter is changed so that the temperature of the flue gas exiting the combustion

chamber is 1400°C, which is influenced by the mass flow of the recirculated flue gas.

Condensation and recirculation side

The stream of the not recirculated flue gas (stream: COLD-FLU), enters a series of compressors and heat exchangers that will separate its water content from the carbon dioxide through condensation. The first compressor, lower pressure C_3, increase the gas pressure up to 1.27 bar, which also increase the temperature. On the other hand the second compressor, higher pressure C_4, increase the pressure up to 1.95 bar (between the two compressors the gas is cooled down).

For calculation purposes, both the two heat exchangers, following the two compressors, instead of a proper heat exchanger Aspen HeatX, are represented by a couple of Aspen Heaters that exchange heat by means of an Aspen heat stream. The bottom heater (hot side) extract the heat from the flue gas and the heat stream brings it to the top heater (cold side). The two hot side heaters (heaters $LP - HX_F$ and $HP - HX_F$) with negative duty, reduce, in both cases, the flue gas temperature down to 94°C and cede the extracted heat through the heat streams (H_1 and H_2).

Before exiting the cycle the flue gas exchange heat with the water stream of the low pressure Rankine cycle in an Aspen HeatX (H-REC). The water stream in question is the "pressurized" (0.75 bar) water stream before the separation, this increase the Rankine cycle's water temperature, increasing the amount of evaporable water in the next heat exchanges, and lower the flue gas' condensing more water.

After every condensation, the liquid water is separated from the remaining gas by means of an Aspen Sep2 separator.

After the last water condensation, the main cycle outlet stream (stream: CO2) exits the cycle in gaseous form and its composition is evaluated.

All the condensed water (streams: $W - COND_{1,2,3}$) is mixed together. This water will enter the high pressure steam turbine and will be injected into the combustion chamber and the HTT. But, before that, the stream mass flow rate has to be adjusted and the water has to be purified and evaporated. The water is evaporated in the HRSG with the heat given by the flue gas exiting the HTT (from the gas turbine side of the cycle). The mass flow of the stream is adjusted depending on the steam demand for the steam injection and the amount of heat that the flue gas can cede. The evaporated water needs to leave the HRSG with a temperature of 550°C. To makes sure of it, a valve FSplit (W-XTRA) removes the water in excess.

After the water in excess is removed (stream: H2O), the impurities are removed with the help of an Aspen Sep (DEAER). The separator acts as the Deaerator that removes the solutes from the condensed water, in the simulation it removes everything that is not water by consuming a small amount of heat.

The purified water (stream: COLD-H2O) enters an Aspen Pump (PUMP), which increase its pressure up to 180 bar. The stream then enters the HRSG where, by receiving the heat coming from the flue gas (stream: POST-HTT), it evaporates. As set in the HeatX, the evaporated water leaves the HRSG at a temperature of 550°C.
Afterwards, the superheated steam (stream: HOT-H2O) enters the high pressure steam turbine (HPT), where it expands until it reaches a pressure of 40 bar. The steam is not expanded until the ambient pressure (which would maximize the power produced by the turbine), because it has to be injected in both the combustion chamber and the gas turbine HTT, reducing the working fluid temperature and increasing its mass flow, hence the power produced in the HTT.
The steam exiting the turbine (stream: LP-H2O), is divided into two sub-streams (streams: COMB-VAP and TURB-VAP) by a splitter (REC-SPLIT). The division is not even. The stream splitting factor is controlled by the design spec (T-HTT) which, by varying the splitting fraction, it makes sure that the mass flow of the steam injected in the turbine (stream: TURB-VAP), is enough to decrease the temperature of the working fluid exiting the gas turbine at a pressure of 1 bar (stream: POST-HTT), down to 573°C.
The valve that removes the water in excess (W-XTRA) is controlled by a design spec as well. The design spec (XTRA-W) calculates the splitting fraction that removes enough water, so that the temperature of the flue gas exiting the HRSG (stream: POST-HRS) is 180°C. The removed water is expelled from the cycle.
To summarize the temperature control, the HeatX HRSG controls the water outlet temperature, while the W-XTRA valve controls the flue gas outlet temperature.

Steam side

As previously said, the condensing heat exchangers of the condensation side (bottom/hot side heaters) provide heat to their cold counterparts (top/cold side heaters). The cold heaters duty is fixed by the thermodynamic content of the flue gas and is transferred to the water of the low pressure Rankine cycle: the steam side of the cycle.
The low pressure cycle operates with super clean feed water, the water purity is important to obtain evaporation and condensation at very low pressure. The water “enters” the cycle (is a closed cycle) with a mass flow of 8.74 kg/s at 22°C and very low pressure: 0.021 bar. It is then immediately pumped up to a pressure of 0.75 bar by an Aspen Pump (PUMP2), it then enters the cold side of the last flue gas condensing heat exchanger H-REC). The heated water is then divided by an Aspen Fsplit (SPLIT) into two sub-streams (streams: W-HT and W-LT). Each of the sub-streams will receive the heat coming from one of the first two condensation process of the flue gas thanks to the heat streams H_1 and H_2. The top sub-stream (stream: W-HT) enters the cold side

heater of the first condensation ($LP - HX_w$) which receives heat from the heat stream H_1.
On the other hand, the bottom sub-stream (stream: W-LT) enters the cold side heater of the second condensation ($HP - HX_w$), which receives heat from the heat stream H_2.
The two superheated streams (streams: W-HT2 and W-LT2) are mixed together once again with an Aspen Mixer. The resulting stream enter a low pressure steam turbine (LPST) with a temperature of 175°C and a pressure of 0.75 bar. In the turbine, the fluid is expanded until it reaches a pressure of 0.021 bar. Afterwards, the super low pressure steam is condensed through an Aspen Heater, which subtract the heat needed to condense the stream by keeping the pressure constant. The temperature of the condensed water (stream: FEED) is 22°C. After being condensed the water is pumped again up to 0.75 bar (by PUMP2), closing the cycle.
Two design specs make sure that the Rankine cycle can operate properly. The first design spec (LP-FEED) controls the mass flow of the water entering the cycle (stream: FEED): it calculates the mass flow needed, to obtain a temperature equal to 175°C at the stream entering the low pressure turbine (stream: PRE-LPST), which is based on the amount of heat that is recovered from the condensation of the flue gas.
The second design spec makes sure that all the water entering the LPST is in vapor phase and that there are no temperature crossovers during the heat exchange between the steam side and the condensation side. To do so, it controls the splitting fraction of the Aspen Split (SPLIT) in order to obtain a temperature of 135°C in the heated bottom sub-stream (stream: W-LT2). This is necessary because the two heat streams, H_1 and H_2, do not carry the same amount of heat (the two dummy heat exchangers have different duty). If this last condition is not implemented, the blocks used could find unreasonable solutions where the cold stream temperature (W-LT2) becomes much higher than the hot stream's that gave up its heat (POST-C4), violating the second law of thermodynamics.

TRANS hierarchy
In order to justify the use of two Aspen Heaters exchanging heat through heat stream, instead of an Aspen HeatX, which better consider the properties of the fluids exchanging heat controlling the feasibility of the process, extra blocks are integrated into the simulation.
As previously said, the use of this dummy heat exchangers during the condensation of the flue gas is purely for calculation purposes: since during the calculations, until the convergence is reached, the hot fluids' mass flow and composition and consequently, their thermal properties, change, it may happen that the HeatX detects a temperature crossover, between the hot and the cold fluids' T-Q curves, before their final properties are set. Therefore finding errors for fluids that are not actually present in the solution: when

convergence is reached. This dummy system prevents this kind of errors and make the simulation converge without issues.
To prove the validity of this method, four Aspen Transfer blocks (one each stream involved), copy the hot and the cold streams' results into other four streams. By selecting "Last" in the transfer block's execute sequence, it is possible to copy the results of the simulated streams and calculate the heat exchange after the simulation is completed (and the calculation error are avoided). The transfer TR-H1 copy the POST-C3 stream into the HOT1 stream; transfer TR-H2 copy the results of POST-C4 into the HOT2 stream; transfer TR-C1 copy the W-HT into the COLD1 stream; TR-C2 copy the W-LT into the COLD2 stream.
The Fig. 5 shows the AspenPlus flowsheet of the base-case model, differently from the Fig. 3 (principle flow scheme of the cycle), the colours do not represent different sides of the cycle, but are meant to differentiate the streams based on their chemical composition and state phase. In addition, the streams thickness tries to gives a relative reference for the streams mass flows (especially for the separation and split units). In detail, the green streams represent the flue gas streams, after each condensation, as the water content diminish, the colour becomes lighter, until the outlet becomes red. All the water streams are of the colour blue, dark blue streams represent condensed water, while the light blue represent stream. As an example of streams thickness, the REC1 stream is thicker than COLD-FLU, this is because the mass flow recirculated is greater than the one condensed. However, the reference is relative because, as an example, the first condensed water stream (W-COND1) obviously has a smaller mass flow, but is made thicker than COLD-FLU.

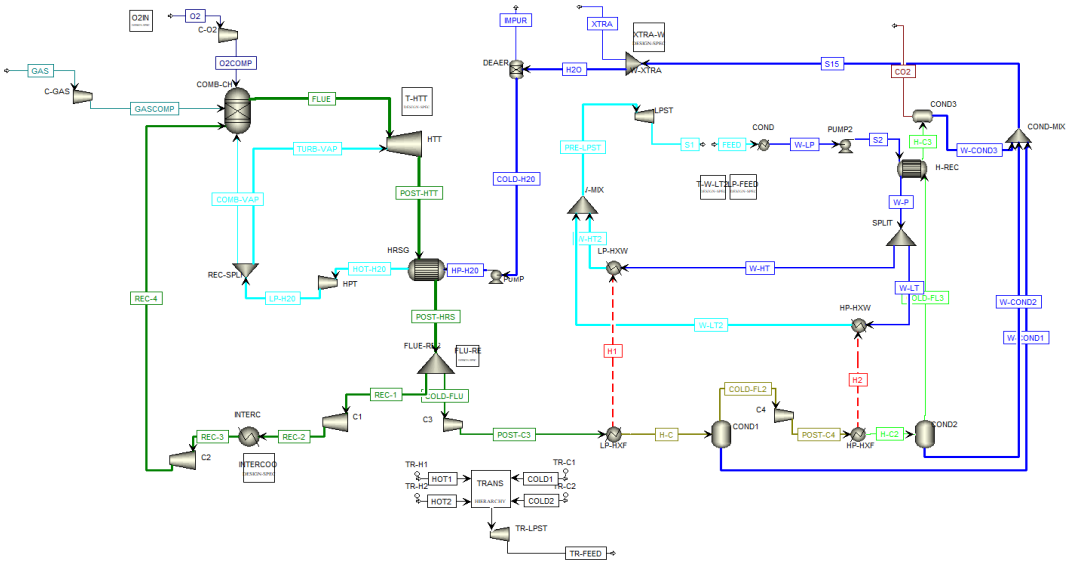

Fig. 5. Base-case flowsheet

3.3.1 Design improvements

There are many ways to possibly improve the cycle performances and optimize the resources usage.
In this work 4 possible improvements are considered:

1. Two shaft configuration.
2. Double-stage HTT.
3. Enhanced heat exchange
4. District heating.

In this work the improvements are considered in succession and not independently, therefore an improvement contains all the previous improvements. For example, District heating improvement model also consider the double-stage HTT improvement, but not vice versa.
The two shaft configuration consist into arranging the gas turbine components on two shafts: the power shaft and the compression shaft. The power shaft is linked to the generator and is responsible for the energy production, the compression shaft is instead connected to the two flue gas compressors C_1 and C_2. These two compressors work with high compression ratio of high temperature flue gas, therefore require great amount of energy. By mechanically connecting the compressors to the turbine, they run at the same rotation al speed. Therefore, the required energy for the compressor is immediately given by the turbine and does not have to be converted, as a result the mechanical losses of the compressors can be neglected. This connection would actually require a multi-stage turbine to actually separate the shaft, but in this work the turbine is assumed single-stage. Since the turbine is assumed single-stage, the Aspen model does not require any modifications.
The double-stage HTT improvement consist into transforming the HTT into a double-stage turbine in order to inject the steam at a lower pressure. In this model the gas turbine is divided into two turbines (HTT and HTT2), the first one expands the mixture coming from the combustion chamber to the pressure of 14 bar, while in the second the steam is injected and expands down to 1 bar. The steam injected in the turbine is not at 40 bar anymore, but at 14 bar as well. A second steam turbine (HPT2) expands the steam from 40 bar to 14 bar. Fig. 6 represent the AspenPlus flowsheet of the double-stage HTT improvement.

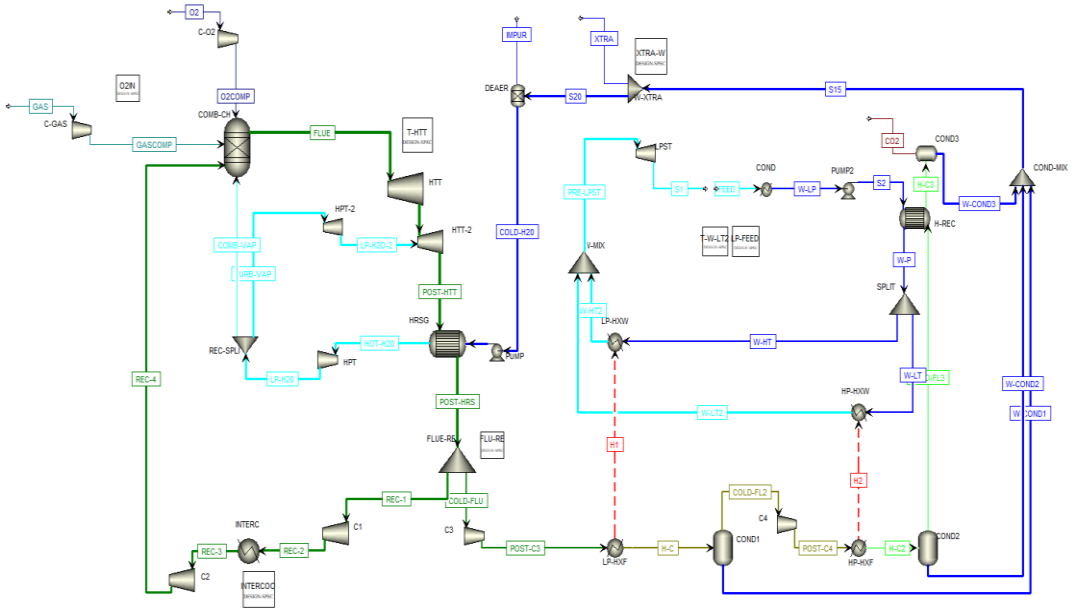

Fig. 6. Double-stage HTT model flowsheet

The improvement goal is not to produce more power in the gas turbine. Respect to the base case, the injected steam has lower temperature (effect of the lower pressure). Lower temperatures mean less steam needed to cool the flue gas down to 573°C (as imposed by the T-HTT design spec). The overall quantity of injectable steam does not change (because controlled by XTRA-W design spec, based on the same 573°C that remain constant), but the quantity injected in the turbine decrease. Therefore, the quantity of steam injected in the combustion chamber increases, as a chain reaction, with more vapour in the combustion chamber there is less need of recirculated flue gas to keep the combustion temperature in check. As a result, the compression work of C_1 and C_2 decreases improving the efficiency of the plant.

The addition of two new turbine (HTT2 and HPT2) increases the efficiency, but does not affect the amount of power produced.

The third improvement, the enhanced heat exchange model, works in a similar way. By improving the overall heat exchange in the HRSG, more injectable steam is available and the design temperatures are reached with less flue gas recirculation and compression power. In this configuration the injected water is heated up by the flue gas exiting the HTT (as in the base-model) and by the recirculated flue gas.

The water heating can be divided in four steps, firstly the water receive the heat from the recirculating flue gas before the first compression C1 (step 1), then it cools down all the flue gases (before the separation) down to 180 °C, as imposed by design (step 2). At this point the water has reached a temperature around 356°C and has started to evaporate, it then receive the heat from the intercooler of the recirculating flue gas between the two compressors (C1 and C2), this almost complete the evaporation (step 3). Lastly the

steam is completely evaporated and superheated up to the target 550 °C, by the flue gas exiting the HTT at a temperature of 573°C (step 4). Summarizing the HRSG of the base case is divided into two heat exchangers (steps 2 and 4 of the new heat recovery system), an additional heat exchanger is added before the first compression (step 1) and the intercooling heat is recovered and used the heat the injected water (step 3). The improved heat exchange has two main advantages: the additional recirculating flue gas cooling, reduce the gases temperatures and therefore, the power needed to compress said gases; with the additional heat recovered it is possible to increase the amount of water entering the injection cycle, this improve the performances of the HPT (bigger mass flow) and increases the amount of injectable water.
With all these new heat exchange, the complexity of the loop increases and the use of an Aspen HeatX for all the exchanges requires too much calculations. To shorten the calculation time and avoid convergence problems, the heat exchanges are simulated with two Aspen Heaters and a heat stream (like in the base-case model). Similarly, a new hierarchy block (HX-SERIE) has been built to verify the heat exchanges. It has been verified from the water side of the exchange. Three transfer blocks (with "Last" execute sequence) have been used, they copied the convergence result of the water stream exiting the pump (stream: HP-H2O), the flue gas exiting the gas turbine and entering the recirculating loop (streams: POST-HTT and REC-1 respectively). The heat exchanges are verified by checking the intermediate temperatures of the involved streams, the conditions of the steam entering the HX-HPT and the power it produces (where HX-HPT is a turbine with the same characteristics and discharge pressure of the HPT). Fig. 7 shows the AspenPlus flowsheet of the enhanced heat exchange model, while Fig. 8 and Fig. 9 shows a close-up of the new heat exchange system and the flowsheet of the HX-SERIE hierarchy block respectively.
The intermediate temperatures obtained in the exchanges depend on the duty given by the hot streams (for example in the intercooler) or are obtained by means of trial and error until there was no more temperature crossover in the hierarchy block. Therefore further exchange optimization could be achieved.

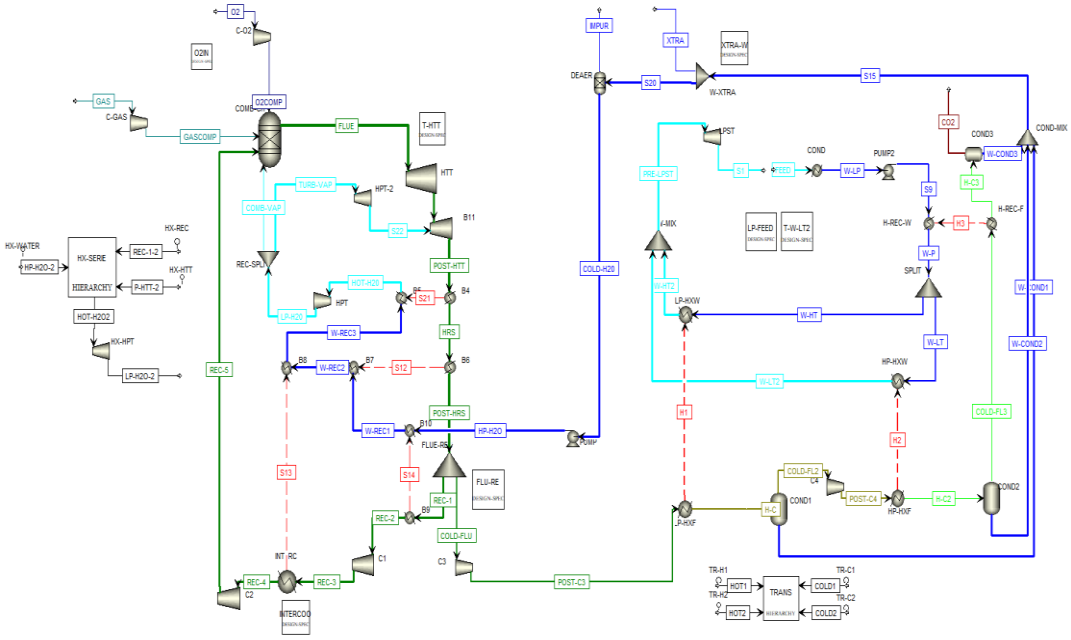

Fig. 7. Enhanced heat exchange model flowsheet

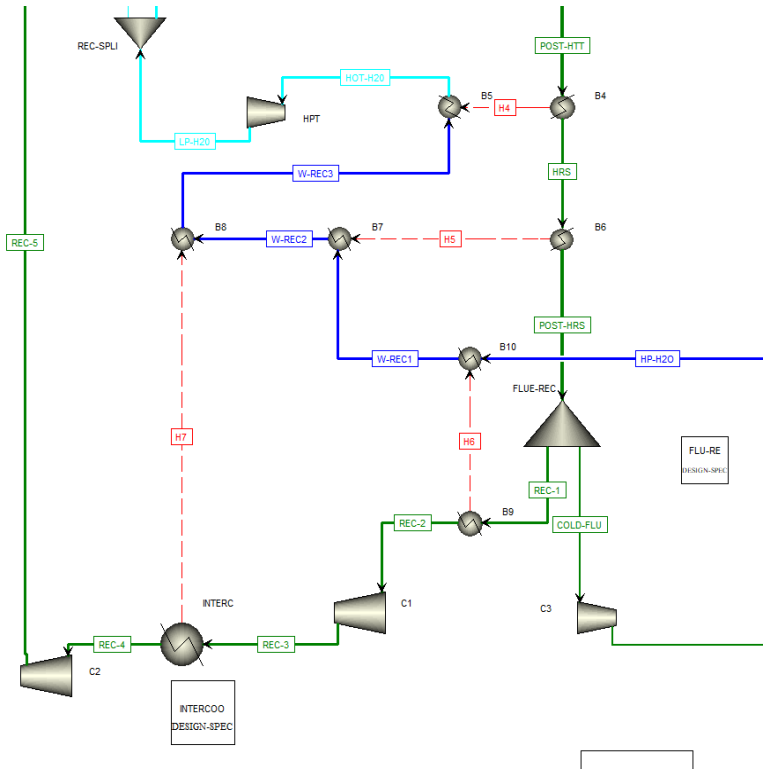

Fig. 8. Enhanced heat exchange close-up

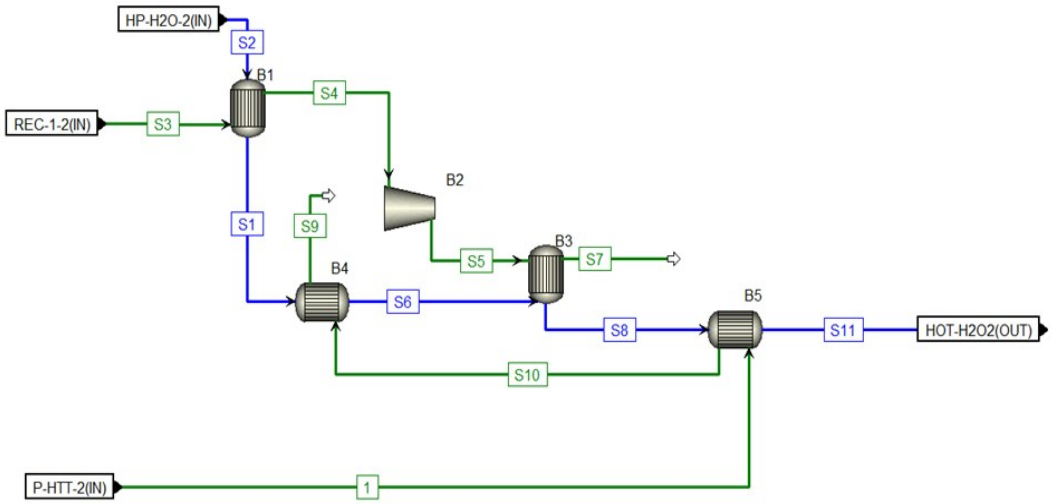

Fig. 9. HX-SERIES hierarchy flowsheet

The last improvement analysed does not focus on the gas turbine side of the cycle, but on the low pressure Rankine cycle side. The improvement consists in the coupling of a district heating (DH) system to the S-Graz cycle. In this model the discharge pressure of the LPST turbine is not a design variable anymore, but it is a value controlled by the design spec HOT-SOUR, which varies the discharge pressure until the outlet temperature of the steam is 80°C (hotter than the base-case). Then the hot steam is cooled down until condensation by an external water stream. This water stream conditions are based on the cold feed of a low temperature district heating system. The steam coming out the LPST has very low pressure, therefore it requires lower temperatures to condense. For this reason the DH system chosen is for tap water supply. Tap water systems have the lowest required DH supply temperature [60]. The DH system feed water in a temperature range of 5-15°C and send it back at a temperature between 55°C to 60°C [60]. As for the inlet and outlet pressure the DH system near Bologna has been taken as reference. In a study published by ENEA on said DH, the water feed pressure is of 4 bar, while it is injected into the distribution net at 10 bar and therefore require pumping after the heat exchange [61]. Fig. 10 shows the AspenPlus flowsheet of the DH-case model.

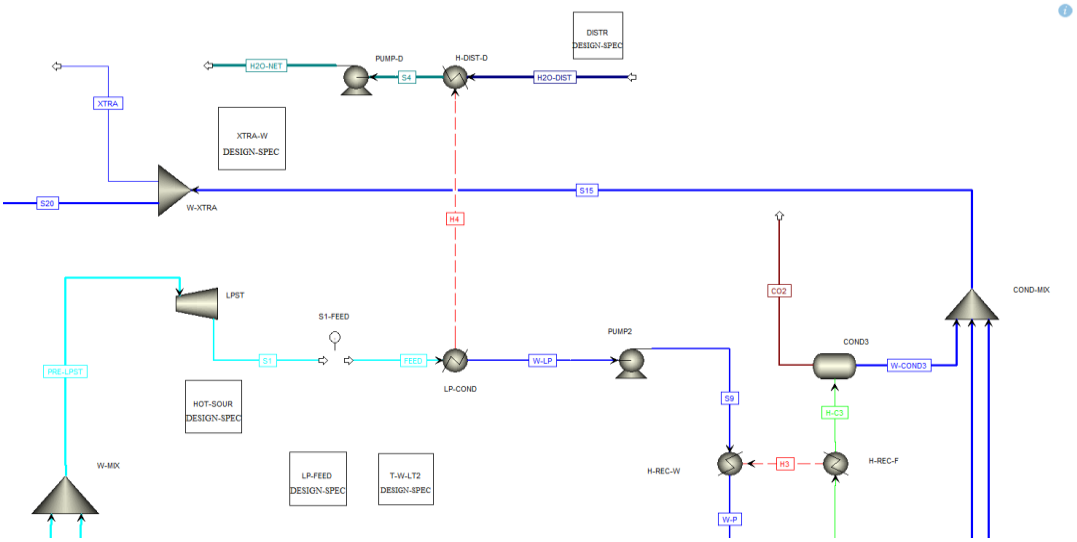

Fig. 10. DH-case model flowsheet

4 Results and discussion

In this section the results of the simulations are presented.
The results focus on the solutions to the convergence of the simulations, the net electrical efficiency of the cycle and the outlet stream composition.

4.1 Convergence solution

With convergence solution physical and numerical results are identified. This section focuses on the calculation of the design specs and on some important streams. Table 6 summarises all the design specs used in the base-case simulations, their target, the varied parameter and its result.

Table 6. Design specs

Design Spec.	Target	Vary	Results
BASE-CASE MODEL			
O2-IN	O2=0,001mol%(FLUE)	O2 mass flow	3.85 [kg/s]
T-HTT	T=573°C (POST-HTT)	REC-SPLI split	0.997
FLU-RE	T=1400°C (FLUE)	FLU-REC split	0.614
INTERCOO	T=580°C (REC-4)	INTERC T_{OUT}	357 [°C]
XTRA-W	T=550°C (HOT-H2O)	W-XTRA split	0.798
LP-FEED	T=175°C (PRE-LPST)	FEED mass flow	8.74 [kg/s]
T-W-LT	T=135°C (W-LT2)	SPLIT split	0.120
DH-CASE MODEL			
DISTR	T=65°C (H2O-NET)	H_20 mass flow	136.75 [kg/s]
HOT-SOUR	T=80°C (S1)	LPST P_{OUT}	0.212 [bar]

The DH-case is the only AspenPlus model that introduces new design spec in the flowsheet. The results present in Table 6 are specific for the base-case model. The calculation done in the other cases are the same, but depending on the model flowsheet they slightly differ.
At the flue gas condensation, the first compressor, lower pressure C_3, increase the temperature up to 206°C. After being cooled down, the second compressor, higher pressure C_4, increase the gas temperature up to 136°C. After each compression, the two hot side heaters (heaters $LP - HX_F$ and $HP - HX_F$) with negative duty, reduce the flue gas temperature down to 94°C and cede the extracted heat through the heat streams (H_1 and H_2). The first temperature decrease removes around 80.8% of the flue gas water content (stream: HC), which corresponds to 61.7% of the total mass flow, while the second cooling removes 10.9% of the (initial) water content, which corresponds to 21.7% of the higher pressure flue gas mass flow (stream: HC-2).

With the last heat exchange (H-REC), the flue gas is further cooled, down to the temperature of 46°C. The water condensed in this last exchange is only 7.7% of the initial amount and corresponds to 19.6% of cooled flue gas mass flow (stream: HC-3).
The condensation efficiency of this process is approximately 99.4%: of the 9.4 kg/s of water in the flue gas that undergoes condensation (stream: COLD-FLU), only 0.06 kg/s are not condensed and exit the cycle (stream: CO2).
After the last water condensation, the main cycle outlet stream (stream: CO2) exits the cycle in gaseous form at a temperature of 46°C. Its composition is mainly carbon dioxide: 85 mol%, argon, molecular nitrogen and water. Given 1.00 kg/s of natural gas at the inlet, the flue gas outlet mass flow is 3.00 kg/s, of which 2.64 kg/s is carbon dioxide.
The condensed water is mixed at a temperature of 90°C. With the XTA-W design spec, 1.89 kg/s of water are expelled, while 7.44 kg/s will be injected as steam. The injectable water, after being pumped, enters the HRSG with a temperature of 94°C. At 40 bar (the injection pressure) the superheated steam has a temperature of 330°C. In the base-case model, approximately all the steam is injected in the turbine (only 0.02 kg/s are injected in the combustion chamber).
In the low pressure Rankine cycle, as previously said, the water feed has a mass flow of 8.74 kg/s and a temperature of 22°C. After exchanging heat in the H-REC, the heated water (stream: W-P) reaches the temperature of 72°C.
The heat streams of the condensation heat exchangers ($HP - HX_W$ and $LP - HX_W$) have different duty with H_1 being much bigger than H_2 (due to the lower condensation heat present in the second condensation stage). Therefore, the mass flows and the temperature reached by the split water streams (W-HT2 and W-LT2) are different. W-HT2 has a mass flow of 7.69 kg/s and a temperature of 180°C, while W-LT2 has a mass flow of 1.05 kg/s and a temperature of 135°C.

4.2 Efficiency analysis

The efficiency of the plant taken into consideration is the net electrical efficiency. Since the simulation calculates the steady-state conditions of the cycle, by considering an operational time, the power generation performances of the S-Graz cycle can be analysed. The time considered is one hour. The efficiency is defined in eq. (1)
eq. 1

$$\eta_{net} = \frac{\sum P_i}{LHV \cdot \rho_{st} \cdot \dot{q}_{st}}$$

In the base-case, the net power produced by the cycle is approximately 18.14 MW. The fuel properties (LHV, standard density and volumetric flow) are calculated by AspenPlus. The efficiency of the base-case model, without

considering the energy consumption for the cryogenic oxygen production and the carbon dioxide storage, is 41.9%.

Table 7 and 8 list the net power of each model component and the fuel characteristics.

Table 7. Base-case components net power

	C-GAS	C-O2	C1	C2	C3	C4	HPT	HTT	LPST	PUMP	PUMP2
P [MW]	0.22	0.43	13.59	8.22	0.56	0.28	-2.36	-35.76	-3.60	0.25	0.001

Green colour and negative values represent power extracted, while positive works and red colour represent power required.

Table 8. Fuel properties

	LHV	ρ_{st}	$\dot{q}_{st}$	P_{ideal}
Base-case fuel	45.54 [MJ/kg]	0.83 [kg/sm^3]	4106.96 [sm^3/h]	43.30 [MW]

To be comparable with other power cycles, the energy consumed by the ASU and to store the carbon, cannot be neglected.
A stream is considered suitable for carbon utilization and storage when its CO_2 concentration is at least 95% [62]. The flue gas obtained in the simulation is not pure enough to be used, or stored, without additional processing. The processing is carried out in a Compression and Purification Unit. In the literature the energy consumption of a CPU, with a target of 95% purity and a feed flue gas of 80% purity, is between 125 and 150 kWh every ton of CO_2 [62], [63]. Based on the flue gas composition obtained in this work, the energy consumption has been assumed equal to 135 $\frac{kWh}{t}$. Table 9 shows the flue gas composition of the base-case.

Table 9. Flue gas composition

	O2	N2	H2O	CO2	AR
mol%	0.6%	3.1%	4.5%	85.0%	6.8%

When the energy consumed for the production of the oxygen stream and the purification of the flue gas are considered, which is equal to 4.75 MW, the efficiency of the cycle drops down to 30.9%.
The efficiency level of the base-case model is well below CCGT level.

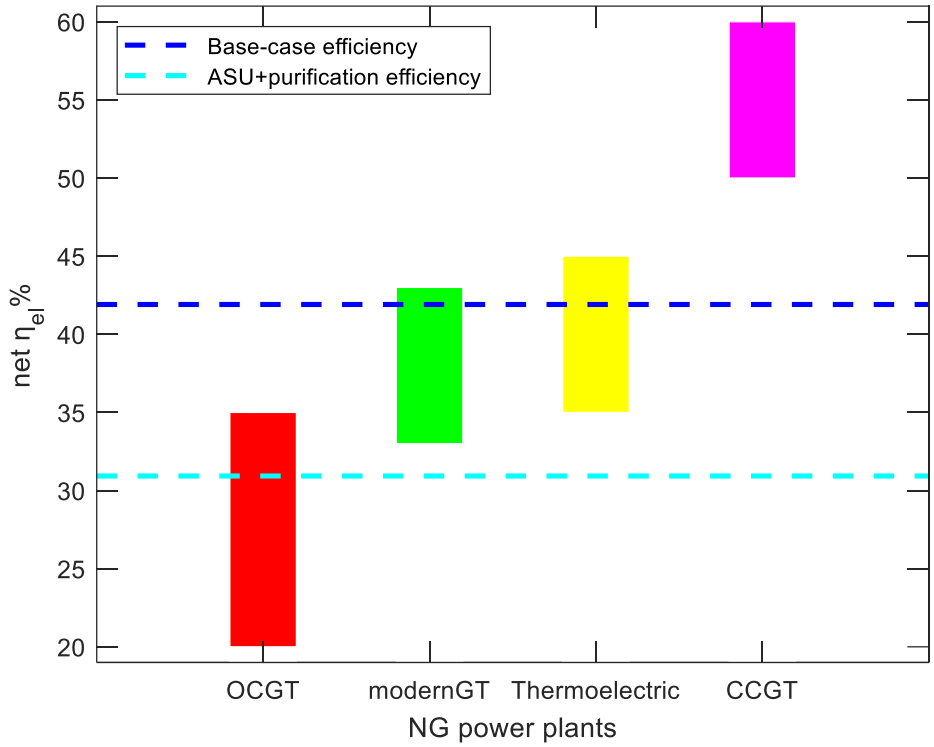

Fig. 11. Comparison between cycle efficiency results and efficiency of commercial NG power plant

To increase the cycle efficiency, improvements have been analysed. This work does not focus on design variables optimization, but analyses the effect of cycle layout changes on efficiency, while still considering the working conditions assumptions coming from previous works, used in the base-case (Table 3,4,5) [55].

It is observed that the greatest source of power consumption, is the compression work of the recirculating C_1/C_2 series (Table 7). Therefore the improvements mainly focus on reducing the recirculating mass flow rate.

As previously said, the improvements considered are four: double-turbine; enhanced heat exchange; district heating; mechanical connection of turbine and compressor (shaft assumption). Fig.12 shows and compare the efficiency obtained in all the simulations. The first result (the first bar) is the net electrical efficiency of the cycle without taking into account the energy required from the oxygen production and the flue gas purification, which is then taken into account in the second result. The third and the fourth are the application of the shaft assumption to the first and the second results.

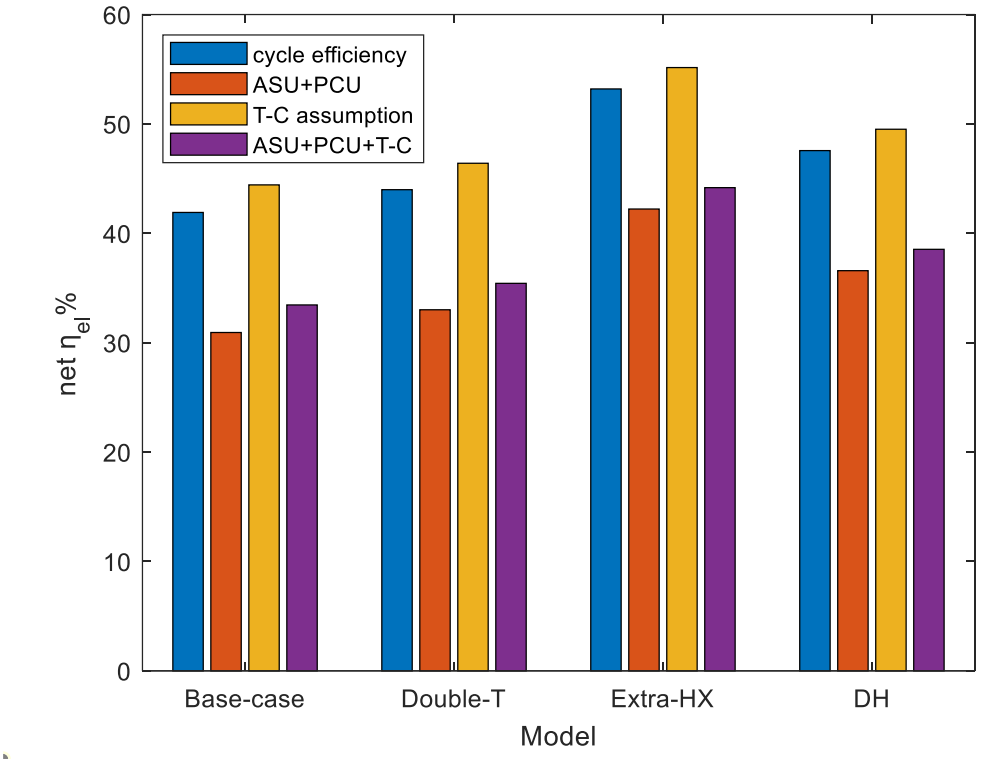

Fig. 12. Models efficiency comparison

It is noticeable that the enhanced heat exchange model (Extra-HX) is the one that bring the greatest net electrical efficiency increase (considering that are not independent models, but consecutive evolutions). This is because it is the model with the biggest water injection mass flow and the smallest flue gas recirculation. Fig.13 and 14 respectively show the dependence of the compression work with the net electrical efficiency and of the recirculated mass flow with the compression work.

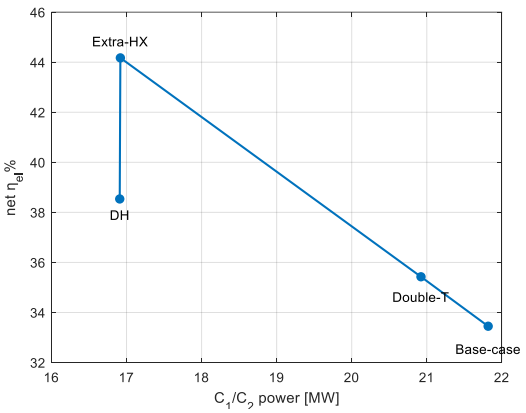

Fig. 13. Efficiency as a function of the compression work

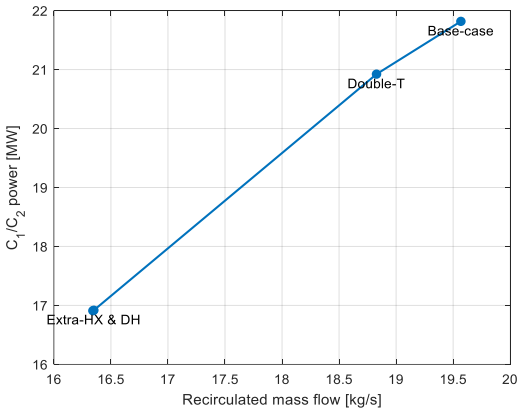

Fig. 14. Relationship between recirculated mass flow and compression work

The efficiency used is the final one (ASU+CPU+T-C), to each dot corresponds a result from one of the models. In Fig. 14 the simulations (dots) are only three because the recirculated mass flow in the HX and DH case are the same. However the net electrical efficiency is different because the steam of the LPST is extracted before it is fully expanded.
In all the models the combustion take place with the same amount of gas and, as consequence, the same amount of oxygen. In addition the flue gas composition remains basically unchanged, therefore the power demand of the ASU and CPU is constant in all the models. The ASU and CPU power demand reduce the efficiency of approximately 11.0% (in all the models).
The shaft assumption neglects the power losses coming from the compressors C_1 and C_2. The compressors' losses are related to their power consumption which is a function of the amount of flue gas recirculated (as shown in Fig.14). Therefore, while the assumption obviously bring efficiency increase to every model, its effect is not equal in all the cases and is most effective in the base-case model, where the flue gas recirculated is at its maximum.

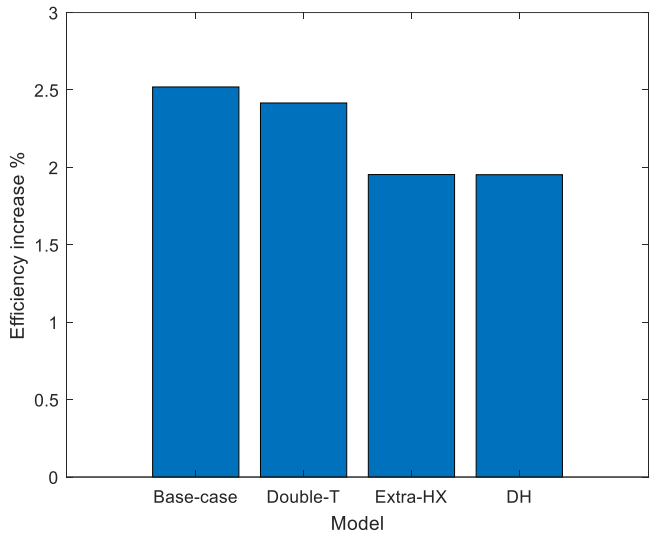

Fig. 15. Shaft assumption effect on the efficiency

The maximum final net electrical efficiency (ASU+CPU+T-C) obtained is from the HX model and is approximately 44.2%.
In order to appreciate the performances of the DH model the cogeneration efficiency is used. The formula used for the cogeneration efficiency (eq.2) is the same as the net electrical efficiency one (eq.1), but also consider the heat generated by the plant, in this case recovered and given to the district heating system.

eq. 2

$$\eta_{cog} = \frac{\sum P_i + Q_{net}}{LHV \cdot \rho_{st} \cdot \dot{q}_{st}}$$

The values of lower heating value, standard density and volume flow, as well as net electrical power ($\sum P_i$) are the same as the electrical efficiency calculation. The power consumed by the pump of the DH system (PUMP-D) was already considered in the net electrical efficiency calculation. Since other than the fuel combustion energy, no other heat is introduced, Q_{net} is the heat that the cycle cede to the DH system. As calculated by DISTR design spec (Table 6), the water mass flow is equal to 136.75 kg/s. The stream is pressurized up to 10 bar by PUMP-D (which consumes 0.10 MW) and receives (from the LPST outlet), through the heat stream H_4, approximately 25.99 MW of heat. Generally the heat recovery from gas turbines does not cause electrical power losses [64]. In this case, to perform the exchange with the DH system, the cycle has been modified so that the discharge pressure of the LPST is higher than HX model's. This cause an electrical power loss of 2.35 MW.
With the given assumptions, the cogeneration efficiency of the DH model is 98.5%. The other models do not produce heat, therefore their cogeneration efficiency is assumed equal to their net electrical efficiency. The heat sinks of the other models (compressors intercooler and/or LP Rankine condenser) may also be totally or partly recovered, but these solutions have not been analysed in this work.

4.3 Fuel effect

In this section the effect of inlet natural gas purity has been analysed. Gas purity means higher methane concentration. A purer gas means less undesired products (NO_x) and stronger combustion. A stronger combustion cause higher temperature, which increase the power extracted by the turbine, but also require bigger flue gas recirculation (stronger cooling).
Other than the base-case inlet gas, the effect of three new gas has been studied and their composition and properties are listed in Table 10 and Table 11 respectively.

Table 10. Inlet gas composition [mol%]

	Base-case	Gas91	Gas95	Gas100
CH_4	85.0	91.3	95.0	100.0
C_2H_6	5.0	5.0	3.3	//
C_3H_8	3.0	1.8	1.2	//
C_4H_{10}	3.0	1.0	0.5	//
CO_2	2.0	0.5	//	//
N_2	2.0	0.4	//	//

Table 11. Inlet gas properties

	LHV [MJ/kg]	ρ_{st} [kg/sm^3]	$\dot{q}_{st}$ [sm^3/h]	P_{ideal} [MW]
Base-case	45.54	0.83	4106.96	43.30
Gas91	48.59	0.76	4518.47	46.17
Gas95	49.70	0.72	4731.74	47.22
Gas100	50.03	0.68	5029.62	47.52

The effect has been studied on the base-case model. As for the model improvements, the design variables are kept constant. The results show that, as the fuel become purer, the increase in power extracted by the HTT, is bigger than the increase in compression work for the recirculation ($\sum P_i \uparrow$). However, it does not results in a tangible efficiency increase, due to the higher LHV of the fuel, which increase the power that can be ideally obtained from it. Thereby the cycle performances are not particularly affected by the fuel quality. Fig. 16 summarises the results obtained by the base-case model with the different gases, while Fig. 17 represent the difference between the variables obtained with a gas of a certain purity and the gas with the successive purity.

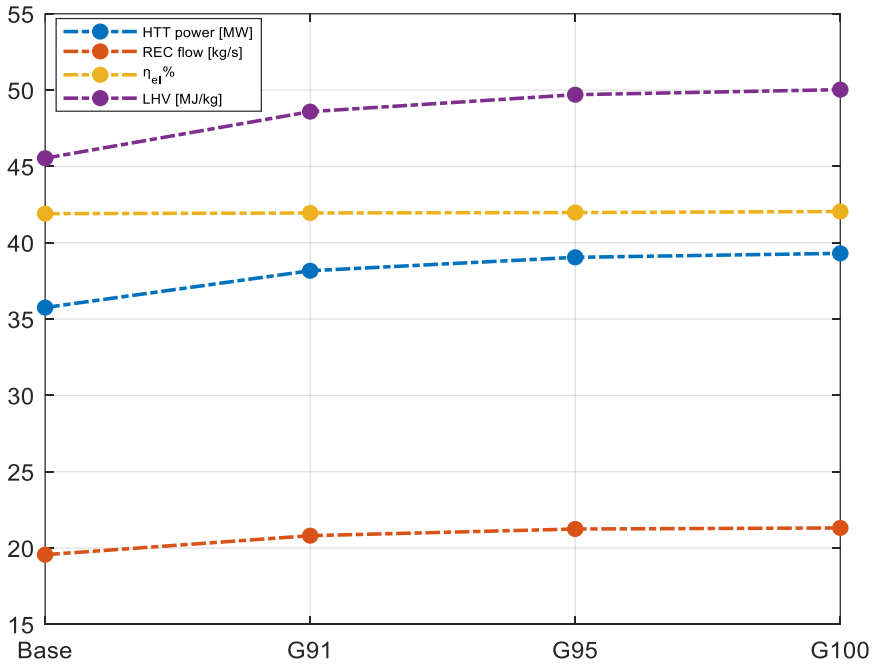

Fig. 16. Parameters evolution changing fuel purity

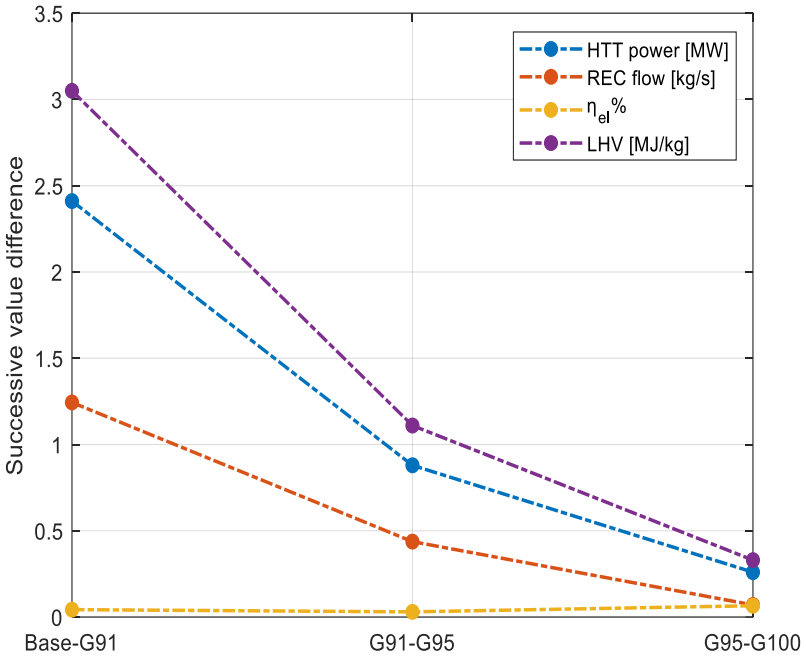

Fig. 17. Parameters successive difference

As shown by Fig. 17, as the gas becomes purer, the effect is less noticeable. The net electrical efficiency considered is the one characteristic of only the cycle, which does not include neither the power consumption of the ASU and CPU, nor the T-C shaft improvement. The choice is caused by minimal efficiency differences when ASU and CPU power demand are considered. A gas with less impurities requires more comburent to complete the combustion, this also results in a higher purification demand (the amount of CO_2 produced increases, but its molar fraction in the flue gas remains constant). G100 requires, for ASU and CPU, 0.41 MW more than the Base fuel. However, when these demand are considered (ASU+CPU eff.), difference between the electrical efficiency of the Base fuel and the G100, increments of only 0.1% (respect to cycle eff.).

For the full methane gas (G100) a particular cycle improvement has been considered. Differently from all the improvements studied this far, this one modify a design variable. Both G95 and G100 present no impurities, but for this simulation G100 has been selected due to its higher LHV. This improvement aims to better exploit the gas purity of the fuel.

The model for reference is the Base-case model. The stream inlet are the G100 (1 kg/s) fuel and an oxygen stream of 100% purity. The new inlet streams completely eliminate the presence of impurities. Therefore the combustion products are exclusively CO_2 and H_2O. In this model, almost all the design spec active in the Base-case simulation are used. The exceptions are the FLU-RE and the T-HTT. FLU-RE, which previously controlled the recirculated flue gas mass flow in order to obtain a combustion chamber outlet temperature of 1400°C, is deactivated and the splitting mass fraction (FLUE-

REC block) of the recirculated gas is set at 0.450 (now the recirculated mass flow is lower than the condensed one). T-HTT does not control the HTT outlet temperature anymore, but the inlet one, previously done by FLUE-REC. The complete absence of impurities avoid the risk of NO_x generation with high temperature, therefore T-HTT fix the combustion temperature up to 1650°C. Lastly the turbine outlet temperature is not controlled anymore. The model is named G100-1650. Table 12 summarize the design spec differences between the Base-case model and the G100-1650.

Table 12. Design spec modifications

Design spec	Target	Vary	Results	Target	Vary	Result
	Base-case			**G100-1650**		
T-HTT	T=573°C (POST-HTT)	REC-SPLI split	0.997	T=1650°C (FLUE)	REC-SPLI split	0.635
FLU-RE	T=1400°C (FLUE)	FLU-REC split	0.614	//	//	//

With the new specifications the injected steam enters the combustion chamber and the turbine with a mass flow of 3.00 kg/s and 5.21 kg/s respectively. Without any constraints on the turbine outlet temperature, the flue gas and injected steam enter the HRSG at 729°C. With less recirculated mass flow the flow entering the HTT decreases and its power generated drops of approximately 7.07 MW respect to the G100 case (the most productive and efficient among the Base-case models). However, at the same time the compression work decreases as well, of 11.71 MW. As a result the net electrical efficiency of this cycle is 52.0% (approximately 10% higher than G100 case's). The performances of the G100-1650 model are compared with the Base and purest gas (G100) models ones in Fig. 18.
Unfortunately, this cycle requires extremely pure inlet streams. Without even considering the power that would be required to purify the NG stream (to obtain 100% purity of methane), at the moment, the only commercially available technology, that can assure such oxygen purity, is electrolysis and it requires far too much energy. Even if electrolysis capacity production (t/day) problem is neglected, the current power requirements is far too high (between 4300 and 6500 $\frac{kWh}{t_{O_2}}$) [51]. Considering a medium value of 5000 $\frac{kWh}{t_{O_2}}$, it would require a power demand of 72.05 MW, making the cycle absolutely inefficient. However, if in the future, the energy demand for oxygen production through electrolysis will decrease greatly, the G100-1650 cycle will be an extremely valid solution. Especially considering that model improvements can further increase its efficiency and that it would not even need a CPU to purify the flue gas CO_2.

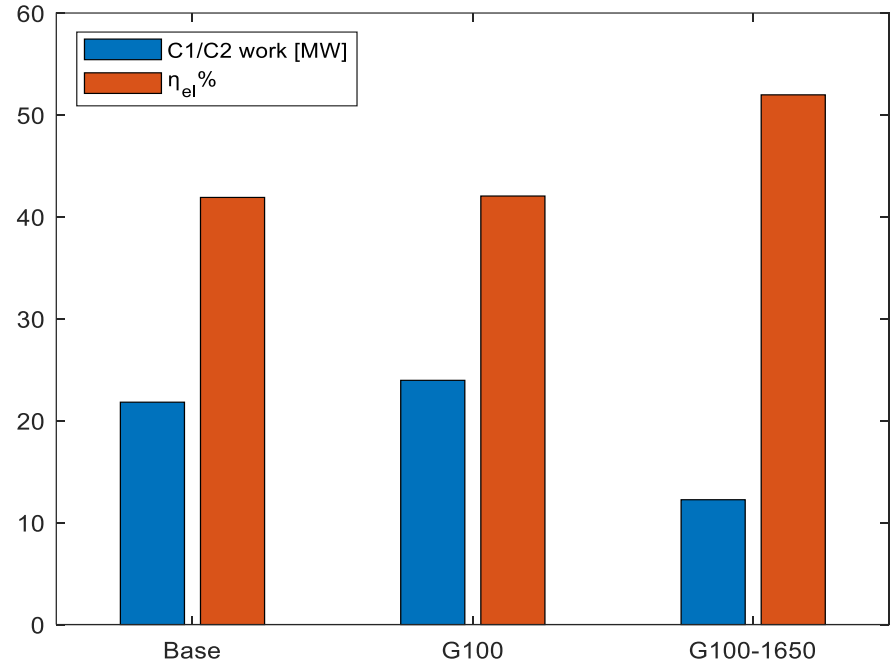

Fig. 18. Comparison of the compressors work and the net electrical efficiency of the G100-1650 case with the G100 and the Base cases.

5 Conclusion

In this work, the climate change problem caused by the Green House Gas emission was explored. The European Union proposed targets on reducing these emissions, that Italy, as a member state, has to meet. In particular, the study focused on the Italian energy sector and the heat and power generated from natural gas. To solve the emissions problem while considering the Italian resources and infrastructures, the modified S-Graz cycle was proposed. The S-Graz cycle is a particular CCGT, with flue gas recirculation and steam injection, running with the oxy-fuel combustion of natural gas and with an high water content in the working fluid. To investigate the performances of such cycle, a steady-state analysis with AspenPlus model was performed. Perfect flow control and zero pressure losses in the components were assumed, in addition the Peng-Robinson equations of state were used to calculate the streams conditions. For the combustion reagents, a natural gas, of composition based on the European gas pipeline standards, and an oxygen stream, of 95% purity produced by a conventional cryogenic double-column ASU, were used. The results obtained by the model showed that the flue gas mostly contained carbon dioxide, argon, water and molecular nitrogen. The molar fraction of the carbon dioxide was high enough (85%) for the flue gas to be eligible for purification (>80%). The cycle net electrical efficiency obtained, considering the energy required by the ASU and the CPU, was 30.9%, lower than the efficiency threshold of 36-39% set by the EU Green Deal. It was observed that the biggest source of power consumption was the compression series of the recirculated flue gas. To reduce the consumption and increase the efficiency three new models were analysed. The new models showed that with the implementation of mechanically driven compressors, steam injection at lower pressures and enhanced heat recovery within the cycle, a net electrical efficiency of 44.2% can be obtained. Furthermore, it was proven that, by modifying the turbine outlet pressure of the low pressure Rankine cycle, the condensation heat can be used as hot source for a tap water DH system obtaining a cogeneration efficiency of 98.5%. Afterwards, the effect of the methane purity in the fuel was studied. Other than the gas composition originally used, the cycle performances were studied with three other fuel composition. The methane purity in the new gases were 91%, 95% and 100%. In this case the results showed that, with the given operating conditions, both the power produced by the turbines and the power consumed by the compressor increased, with the turbine power increasing fairly more. However, due to the fuel properties, it was obtained that the fuel purity does not affect the cycle efficiency. Lastly, the cycle operating conditions were modified to better exploit the gas purity and increase its efficiency. In this model both the methane and oxygen purity were set to 100%. The efficiency obtained without considering feed purification was 52.0%. However with the current technologies, when the oxygen purification is considered, the cycle consumes more power that it can produce.

Looking at the efficiencies, the S-Graz cycle can only match the efficiency of an OCGT. When the improvements considered are implemented, the cycle surpasses the efficiency of both the OCGTs, the modern gas turbines and most of the thermoelectric plants, but still cannot reach the performances of conventional CCGT. This could change in the future if the energy demand for oxygen production drops. At the moment, from the energy perspective, Italy should opt for CCGT power plants, but, considering the increasing emissions restrictions and carbon taxations, building/retrofitting into a zero-emission S-Graz cycle could be an advantageous investment. Therefore, an economic analysis on the problem should be performed.

6 References

[1] J. Romero, O. Geden ; Bronwyn Hayward, and F. E. L. Otto, “The Gambia), Aïda Diongue-Niang (Senegal), David Dodman”.

[2] “CO2 Emissions in 2022 – Analysis - IEA.” https://www.iea.org/reports/co2-emissions-in-2022 (accessed Jun. 16, 2023).

[3] H. Mclaughlin *et al.*, “Carbon capture utilization and storage in review: Sociotechnical implications for a carbon reliant world,” 2023, doi: 10.1016/j.rser.2023.113215.

[4] M. Cheng, P. Verma, Z. Yang, and R. L. Axelbaum, “Single-column cryogenic air separation: Enabling efficient oxygen production with rapid startup and low capital costs-application to low-carbon fossil-fuel plants,” *Energy Convers Manag*, vol. 248, pp. 196–8904, 2021, doi: 10.1016/j.enconman.2021.114773.

[5] Q. Fu, Y. Kansha, C. Song, Y. Liu, M. Ishizuka, and A. Tsutsumi, “A cryogenic air separation process based on self-heat recuperation for oxy-combustion plants,” *Appl Energy*, vol. 162, pp. 1114–1121, Jan. 2016, doi: 10.1016/J.APENERGY.2015.03.039.

[6] H. Jericha, W. Sanz, and E. Göttlich, “GT2006-90032 DESIGN CONCEPT FOR LARGE OUTPUT GRAZ CYCLE GAS TURBINES,” 2006.

[7] “Delivering the European Green Deal.” https://commission.europa.eu/strategy-and-policy/priorities-2019-2024/european-green-deal/delivering-european-green-deal_en (accessed Jul. 01, 2023).

[8] “What are the different types of renewable energy? | National Grid Group.” https://www.nationalgrid.com/stories/energy-explained/what-are-different-types-renewable-energy (accessed May 28, 2023).

[9] “What is renewable energy? | United Nations.” https://www.un.org/en/climatechange/what-is-renewable-energy (accessed Jul. 07, 2023).

[10] “Renewable technologies and their geographical location: Why it matters — RatedPower.” https://ratedpower.com/blog/location-renewable-technology/ (accessed Jul. 07, 2023).

[11] Q. Liu, Q. Miao, J. J. Liu, and W. Yang, “Solar and wind energy resources and prediction,” *Journal of Renewable and Sustainable Energy*, vol. 1, no. 4, p. 043105, Jul. 2009, doi: 10.1063/1.3168403.

[12] “The Advantages and Disadvantages of Renewable Energy | EnergySage.” https://news.energysage.com/advantages-and-disadvantages-of-renewable-energy/ (accessed Jul. 07, 2023).

[13] P. Zhou, R. Y. Jin, and L. W. Fan, “Reliability and economic evaluation of power system with renewables: A review”, doi: 10.1016/j.rser.2015.12.344.

[14] “U.S. Energy Information Administration - EIA - Independent Statistics and Analysis.” https://www.eia.gov/todayinenergy/detail.php?id=42915 (accessed Jul. 07, 2023).

[15] “Total Load - Terna spa.” https://www.terna.it/en/electric-system/transparency-report/total-load (accessed Jul. 07, 2023).

[16] “Europe – Countries & Regions - IEA.” https://www.iea.org/regions/europe (accessed Jul. 08, 2023).

[17] “Increasing the ambition of EU emissions trading.” https://climate.ec.europa.eu/eu-action/european-green-deal/delivering-european-green-deal/increasing-ambition-eu-emissions-trading_en (accessed Jul. 08, 2023).

[18] “Italy - Countries & Regions - IEA.” https://www.iea.org/countries/italy (accessed Jul. 08, 2023).

[19] “Coal explained - U.S. Energy Information Administration (EIA).” https://www.eia.gov/energyexplained/coal/ (accessed Jul. 11, 2023).

[20] “Low-emission power generation with natural gas | Uniper.” https://www.uniper.energy/about-uniper/business-structure/energy-sales/ues-magazine/low-emission-power-generation-with-natural-gas (accessed Jul. 11, 2023).

[21] “Viaspace : Biomass Versus Fossil Fuels, Solar and Wind.” https://www.viaspace.com/biomass_versus_alternatives.php (accessed Jul. 11, 2023).

[22] “Le Centrali in Italia – Assocarboni.” https://assocarboni.it/assocarboni/il-carbone/le-centrali-in-italia/ (accessed May 28, 2023).

[23] M. Dello and S. Economico, “PIANO NAZIONALE INTEGRATO PER L’ENERGIA E IL CLIMA”.

[24] “ARERA - Consumi di gas naturale per settore.” https://www.arera.it/it/dati/gmconsumi.htm (accessed Jul. 11, 2023).

[25] “Natural Gas Consumption Statistics | Natural Gas Data | Enerdata.” https://yearbook.enerdata.net/natural-gas/gas-consumption-data.html (accessed Jul. 11, 2023).

[26] “Italy Natural Gas Security Policy – Analysis - IEA.” https://www.iea.org/articles/italy-natural-gas-security-policy (accessed Jul. 11, 2023).

[27] “Italy: natural gas supply by origin 2022 | Statista.” https://www.statista.com/statistics/1325804/natural-gas-supply-in-italy-by-origin/ (accessed Jul. 14, 2023).

[28] “Information leaflet 1. General information”, Accessed: Jul. 14, 2023. [Online]. Available: https://ec.europa.eu/energy/en/topics/infrastructure/projects-common-interest

[29] “U.S. Energy Information Administration - EIA - Independent Statistics and Analysis.” https://www.eia.gov/todayinenergy/detail.php?id=54780 (accessed Jul. 14, 2023).

[30] F. Schreiner and M. Riemer, “Conversion of LNG Terminals for Liquid Hydrogen or Ammonia Analysis of Technical Feasibility under Economic Considerations Conversion of LNG Terminals for Liquid Hydrogen or Ammonia Project coordination Responsible for content,” 2022.

[31] K. K. Agrawal, S. Jain, A. K. Jain, and S. Dahiya, “Assessment of greenhouse gas emissions from coal and natural gas thermal power plants using life cycle approach,” *International Journal of Environmental Science and Technology*, vol. 11, no. 4, pp. 1157–1164, Nov. 2014, doi: 10.1007/S13762-013-0420-Z/TABLES/6.

[32] “How Gas Turbine Power Plants Work | Department of Energy.” https://www.energy.gov/fecm/how-gas-turbine-power-plants-work (accessed Jul. 14, 2023).

[33] “Open-cycle gas turbines (2022) | Ipieca.” https://www.ipieca.org/resources/energy-efficiency-solutions/open-cycle-gas-turbines-2022 (accessed Jul. 14, 2023).

[34] “Combined heat and power (2022) | Ipieca.” https://www.ipieca.org/resources/energy-efficiency-solutions/combined-heat-and-power-2022 (accessed Jul. 14, 2023).

[35] “Combined-cycle gas turbines (2022) | Ipieca.” https://www.ipieca.org/resources/energy-efficiency-solutions/combined-cycle-gas-turbines-2022 (accessed Jul. 14, 2023).

[36] A. Bhavsar, D. Hingar, S. Ostwal, I. Thakkar, S. Jadeja, and M. Shah, “The current scope and stand of carbon capture storage and utilization ~ A comprehensive review,” 2023, doi: 10.1016/j.cscee.2023.100368.

[37] R. K. Sahoo and S. Gu, “4E analysis of the cryogenic CO 2 separation process integrated with waste heat recovery,” 2023, doi: 10.1016/j.energy.2023.127922.

[38] S. Sani, X. Liu, L. Stevens, H. Wang, and C. Sun, “Amine functionalized lignin-based mesoporous cellular carbons for CO2 capture,” *Fuel*, vol. 351, p. 128886, Nov. 2023, doi: 10.1016/J.FUEL.2023.128886.

[39] T. E. Akinola, P. L. Bonilla Prado, and M. Wang, “Experimental studies, molecular simulation and process modelling \simulation of adsorption-based post-combustion carbon capture for power plants: A state-of-the-art review,” 2022, doi: 10.1016/j.apenergy.2022.119156.

[40] L. Wu *et al.*, “Capture CO 2 from N 2 and CH 4 by zeolite L with different crystal morphology,” 2021, doi: 10.1016/j.micromeso.2021.110956.

[41] Q. Wang *et al.*, “High temperature adsorption of CO 2 on Mg-Al hydrotalcite: Effect of the charge compensating anions and the synthesis pH,” *Catal Today*, vol. 164, pp. 198–203, 2011, doi: 10.1016/j.cattod.2010.10.042.

[42] T. O. Nelson, A. Kataria, P. Mobley, M. Soukri, and J. Tanthana, “RTI’s Solid Sorbent-Based CO2 Capture Process: Technical and Economic Lessons Learned for Application in Coal-fired, NGCC, and Cement Plants,” *Energy Procedia*, vol. 114, pp. 2506–2524, Jul. 2017, doi: 10.1016/J.EGYPRO.2017.03.1409.

[43] M. Younas *et al.*, “Post-combustion CO2 capture with sweep gas in thin film composite (TFC) hollow fiber membrane (HFM) contactor,” *Journal of CO2 Utilization*, vol. 40, p. 101266, Sep. 2020, doi: 10.1016/J.JCOU.2020.101266.

[44] L. Hu, K. Clark, T. Alebrahim, and H. Lin, “Mixed matrix membranes for post-combustion carbon capture: From materials design to membrane engineering,” *J Memb Sci*, vol. 644, p. 120140, Feb. 2022, doi: 10.1016/J.MEMSCI.2021.120140.

[45] N. Prasetya, N. F. Himma, P. D. Sutrisna, I. G. Wenten, and B. P. Ladewig, “A review on emerging organic-containing microporous material membranes for carbon capture and separation,” *Chemical Engineering Journal*, vol. 391, p. 123575, Jul. 2020, doi: 10.1016/J.CEJ.2019.123575.

[46] J. Mletzko, S. Ehlers, and A. Kather, “Comparison of Natural Gas Combined Cycle Power Plants with Post Combustion and Oxyfuel Technology at Different CO2 Capture Rates,” *Energy Procedia*, vol. 86, pp. 2–11, Jan. 2016, doi: 10.1016/J.EGYPRO.2016.01.001.

[47] T. Wilberforce, A. Baroutaji, B. Soudan, A. H. Al-Alami, and A. Ghani Olabi, “Outlook of carbon capture technology and challenges,” 2018, doi: 10.1016/j.scitotenv.2018.11.424.

[48] S. C. Gowd *et al.*, “Economic perspectives and policy insights on carbon capture, storage, and utilization for sustainable development,” 2023, doi: 10.1016/j.scitotenv.2023.163656.

[49] H. Mohammadpour, R. Cord-Ruwisch, A. Pivrikas, and G. Ho, “Utilisation of oxygen from water electrolysis – Assessment for wastewater treatment and aquaculture,” *Chem Eng Sci*, vol. 246, p. 117008, Dec. 2021, doi: 10.1016/J.CES.2021.117008.

[50] T. Kato, M. Kubota, N. Kobayashi, and Y. Suzuoki, “Effective utilization of by-product oxygen from electrolysis hydrogen production,” *Energy*, vol. 30, no. 14, pp. 2580–2595, Nov. 2005, doi: 10.1016/J.ENERGY.2004.07.004.

[51] S. García-Luna, C. Ortiz, A. Carro, R. Chacartegui, and L. A. Pérez-Maqueda, “Oxygen production routes assessment for oxy-fuel combustion,” *Energy*, vol. 254, p. 124303, Sep. 2022, doi: 10.1016/J.ENERGY.2022.124303.

[52] R. Stanger *et al.*, “Oxyfuel combustion for CO2 capture in power plants,” *International Journal of Greenhouse Gas Control*, vol. 40, pp. 55–125, Sep. 2015, doi: 10.1016/J.IJGGC.2015.06.010.

[53] H. Jericha, “Graz Cycle-a Zero Emission Power Plant of Highest Effi ciency 1.3.1.1”, Accessed: Jul. 18, 2023. [Online]. Available: http://www.ttm.tugraz.at

[54] K. Wimmer and W. Sanz, “Optimization and comparison of the two promising oxy-combustion cycles NET Power cycle and Graz Cycle,” *International Journal of Greenhouse Gas Control*, vol. 99, p. 103055, Aug. 2020, doi: 10.1016/J.IJGGC.2020.103055.

[55] H. Jericha, W. Sanz, and E. Göttlich, “Design concept for large output Graz Cycle gas turbines,” *J Eng Gas Turbine Power*, vol. 130, no. 1, Jan. 2008, doi: 10.1115/1.2747260.

[56] S. Chen, H. Liu, and C. Zheng, “Methane combustion in MILD oxyfuel regime: Influences of dilution atmosphere in co-flow configuration,” 2017, doi: 10.1016/j.energy.2017.01.011.

[57] R. Kumar Maurya and A. Kumar Agarwal, “Experimental investigation on the effect of intake air temperature and air-fuel ratio on cycle-to-cycle variations of HCCI combustion and performance parameters,” 2010, doi: 10.1016/j.apenergy.2010.09.027.

[58] “$name.” https://www.aspentech.com/en/products/pages/aspen-plusrt (accessed Jun. 09, 2023).

[59] “CONTRACT FOR THE SUPPLY OF FUEL GAS,” 2022.

[60] P. Gummerus, “New developments in substations for district heating,” *Advanced District Heating and Cooling (DHC) Systems*, pp. 215–221, Jan. 2016, doi: 10.1016/B978-1-78242-374-4.00010-0.

[61] M. A. Ancona and F. Melino, “MINISTERO DELLO SVILUPPO ECONOMICO”.

[62] B. Jin, H. Zhao, and C. Zheng, “Optimization and control for CO2 compression and purification unit in oxy-combustion power plants,” *Energy*, vol. 83, pp. 416–430, Apr. 2015, doi: 10.1016/J.ENERGY.2015.02.039.

[63] M. X. Xu, H. B. Wu, Y. C. Wu, H. X. Wang, H. D. Ouyang, and Q. Lu, “Design and evaluation of a novel system for the flue gas compression and purification from the oxy-fuel combustion process,” *Appl Energy*, vol. 285, p. 116388, Mar. 2021, doi: 10.1016/J.APENERGY.2020.116388.

[64] M. Gambini and M. Vellini, “High Efficiency Cogeneration: Performance Assessment of Industrial Cogeneration Power Plants,” *Energy Procedia*, vol. 45, pp. 1255–1264, Jan. 2014, doi: 10.1016/J.EGYPRO.2014.01.131.